Ginzburg Centennial Conference on Physics
29.05.2017

Gravitational Quantum Spectroscopy with Ultracold Particles

GRANIT and GBAR collaborations

Gravitational Quantum Spectroscopy with Ultracold Particles

Gravitational quantum spectroscopy with neutrons

Gravitational quantum spectroscopy with antihydrogen (hydrogen) atoms

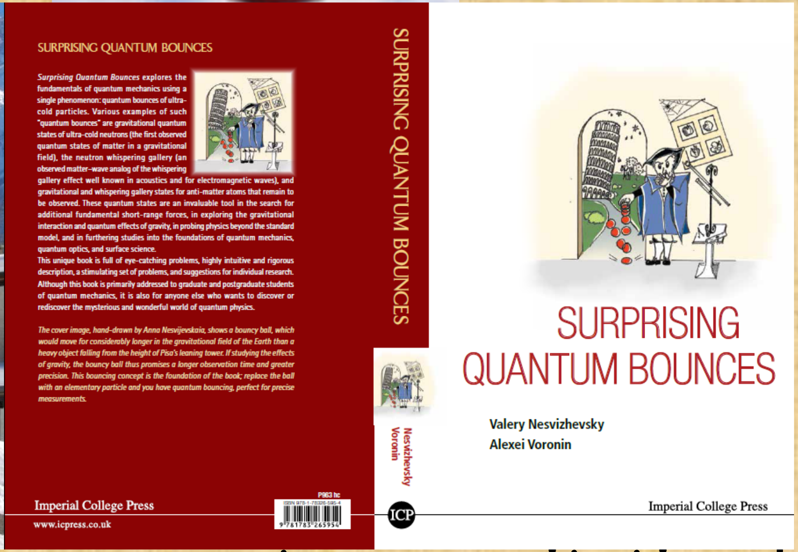

Ultracold systems: quantum gravitational states: 10 nK, ultracold antihydrogen: 100 μK, ultracold neutrons: 1mK

References

Observation of gravitational states of neutrons: [V.V. N., H.G. Boerner, A.K. Petukhov, H. Abele, S. Baessler, F.J. Ruess, T. Stoferle, A. Westphal, A.M. Gagarski, G.A. Petrov, and A.V. Strelkov, *Quantum states of neutrons in the Earth's gravitational field*, Nature 415:297, 2002] and further publications;

Observation of whispering-gallery states of neutrons: [V.V. N., A.Yu. Voronin, R. Cubitt, and K.V. Protasov, *Neutron whispering gallery*, Nature Physics 6:114, 2010];

Proposal to measure gravitational quantum states of antihydrogen atoms: [A.Yu. Voronin, V.V. N., P. Froelich, *Gravitational quantum states of antihydrogen*, Phys. Rev. A 83:032903, 2011] and further publications;

Calculations of quantum reflection of (anti)atoms from the surface ([G. Dufour, A. Gerardin, R. Guerout, A. Lambrecht, V.V. N., S. Reynaud, A.Yu. Voronin, *Quantum reflection of antihydrogen from the Casimir potential above matter slabs*, Phys. Rev. A 87: 012901, 2013] and further publications)

More information in publications of Tokyo, qBounce, GRANIT, GBAR collaborations, in GRANIT workshop proceedings: [GRANIT-2014, *Gravitational Quantum Spectroscopy*, Adv. High En. Phys. 467409:2, 2014]; [*GRANIT-2010*, Compt. Rend. Phys. 12:703, 2011].

NEUTRONS FOR SCIENCE

Gravitational and whispering-gallery quantum states of neutrons

Gravitational and inertial masses

Essential features:

- The mirror is a uniform potential barrier, with no internal structure,
- The particles are reflected from the mirror elastically,
- Ultracold neutrons (UCNs) are the first particles, which provided measurements of such quantum states;
- Ultracold (anti)atoms is the second candidate particle.

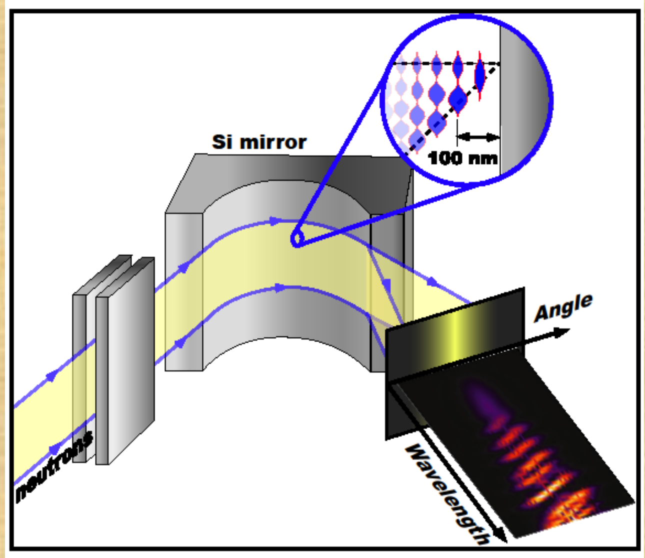

Inertial mass

Ultracold (anti)atoms? Quantum reflection!

Problem: **attractive** van der Waals/Casimir-Polder potential.

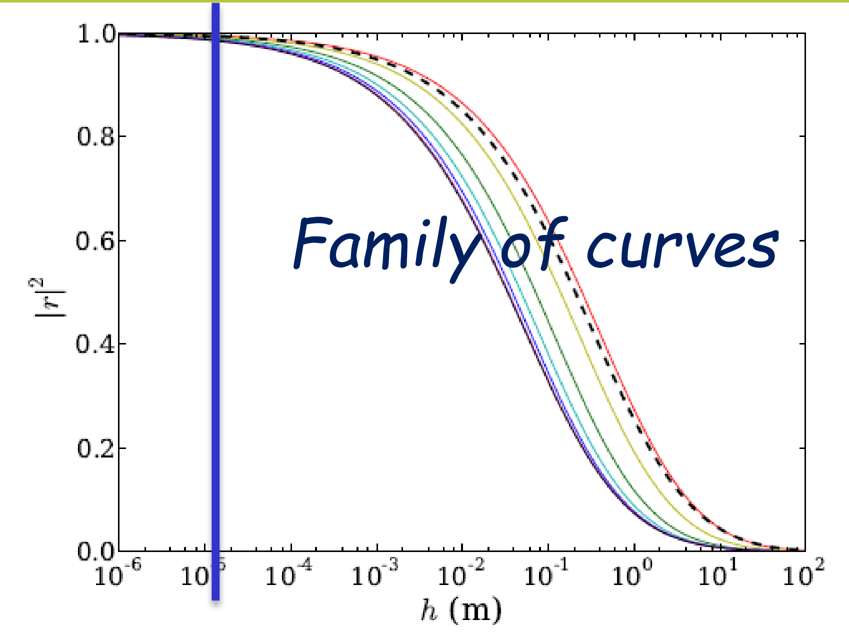

Solution: **Quantum reflection** is the limit of lowest energies (gravitational quantum states!!!) provides nearly total reflection of an atom from a mirror.

Quantum reflection of atoms has been demonstrated experimentally.

G. Dufour et al, *Quantum reflection of antihydrogen from the Casimir potential above matter slabs*, Phys. Rev. A 87, 2013

We have also found materials/conditions, which provide much higher reflectivity – to be published.

Gravity / Acceleration

$$E_n \approx \sqrt[3]{\left(\left(\frac{9 \cdot m_n}{8}\right) \cdot \left(\pi \cdot \hbar \cdot g \cdot \left(n - \frac{1}{4}\right)\right)\right)^2}$$

Gravitational and inertial masses

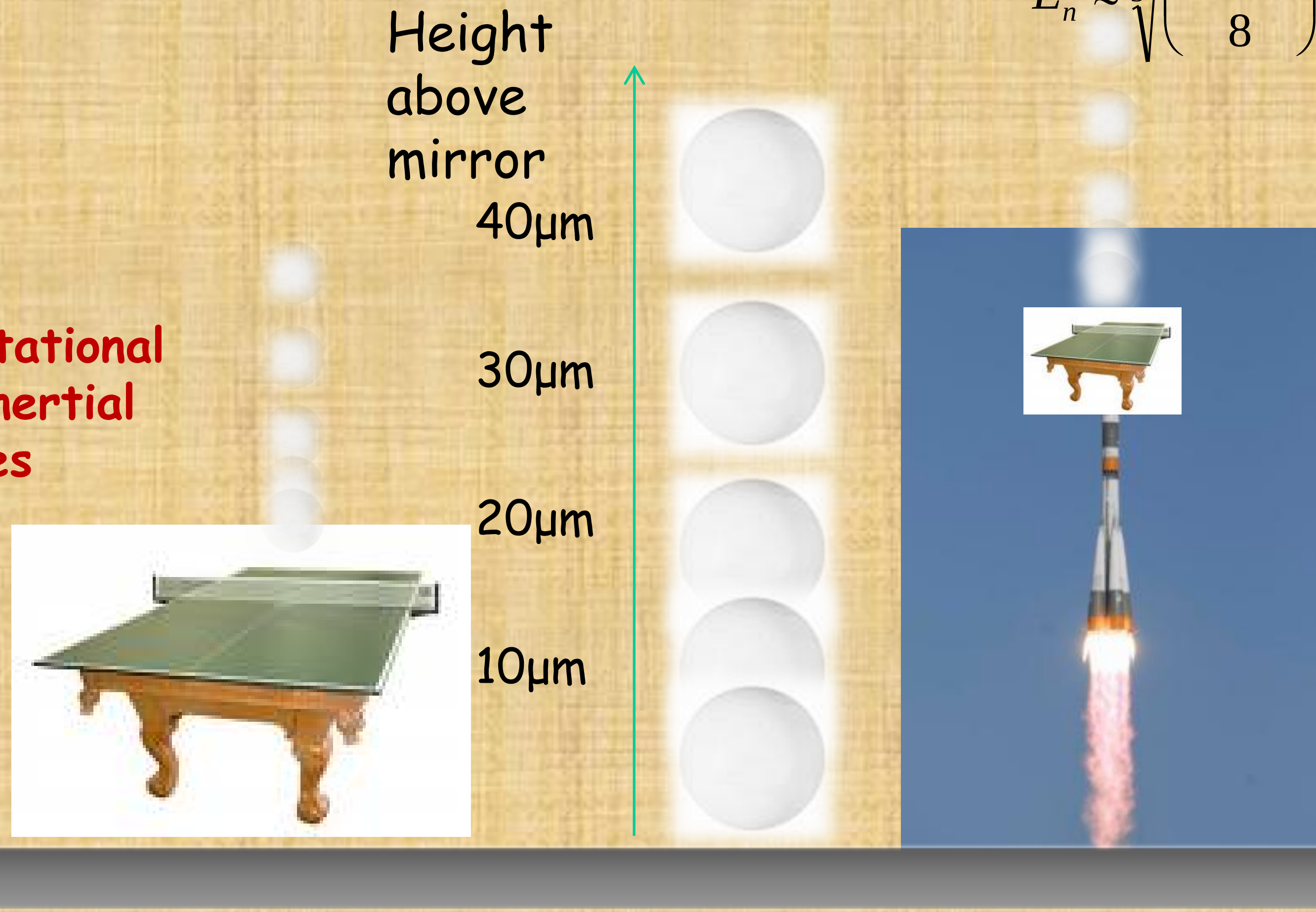

Inertial mass

An illustration for quantum motion of a particle above a mirror in a gravitational field and that in an accelerated frame. The heights of the ball correspond to most probable heights of a neutron in 5th quantum state.

Matter / Antimatter

Gravitational and inertial masses

Gravitational and inertial masses of the antiparticle

? ? ?...

Gravitational properties of antimatter have never been measured directly

An "artistic" illustration for quantum motion of a particle built of normal matter (left) and antimatter (right) in a gravitational field

Gravitational states / Fountains

NEUTRONS FOR SCIENCE

- Observation times are defined by quantum reflection (up to a few seconds)	=	- Observation times are defined by the time of flight in the gravitational field (up to a few seconds)
- Statistics is defined by the phase-space density and the resolution	=	- Statistics is defined by the phase-space density and the resolution
- Compact design	>	- Large sizes
- Dramatic increase of observation times in microgravity environment	>	- Increase of observation times in microgravity environment

1. Gravitational quantum states of particles in a gravitational field is the ultimate limit of particle fountains;

2. The logics of development of interferometric experiments with ultracold neutrons of the previous decades: from fountains to gravitational states;

3. BUT the theoretical predication of large probability of quantum reflections has to be demonstrated experimentally.

Fundamental short-range forces and neutrons

Short-range forces

Phenomenologically:

- Spin-independent,
- Spin-dependent.

Origin:

- Extra light bosons,
- Extra spatial dimensions,
- Dark matter,
- Axion-like particles etc

Neutrons

- Electric neutrality,
- Availability of high fluxes of neutrons with wavelengths comparable to the spatial scale of extra interactions to probe,
- High probability of elastic interaction with matter.

Fundamental short-range forces and neutrons

All measurements with neutrons related to the topic of this talk are performed at the Institut Max von Laue - Paul Langevin (ILL), Grenoble, France. All measurements involve ILL scientists (co-authors of relevant publications) and also all measurements use various ILL facilities (GRANIT, PF1B, PF2, D17 etc).

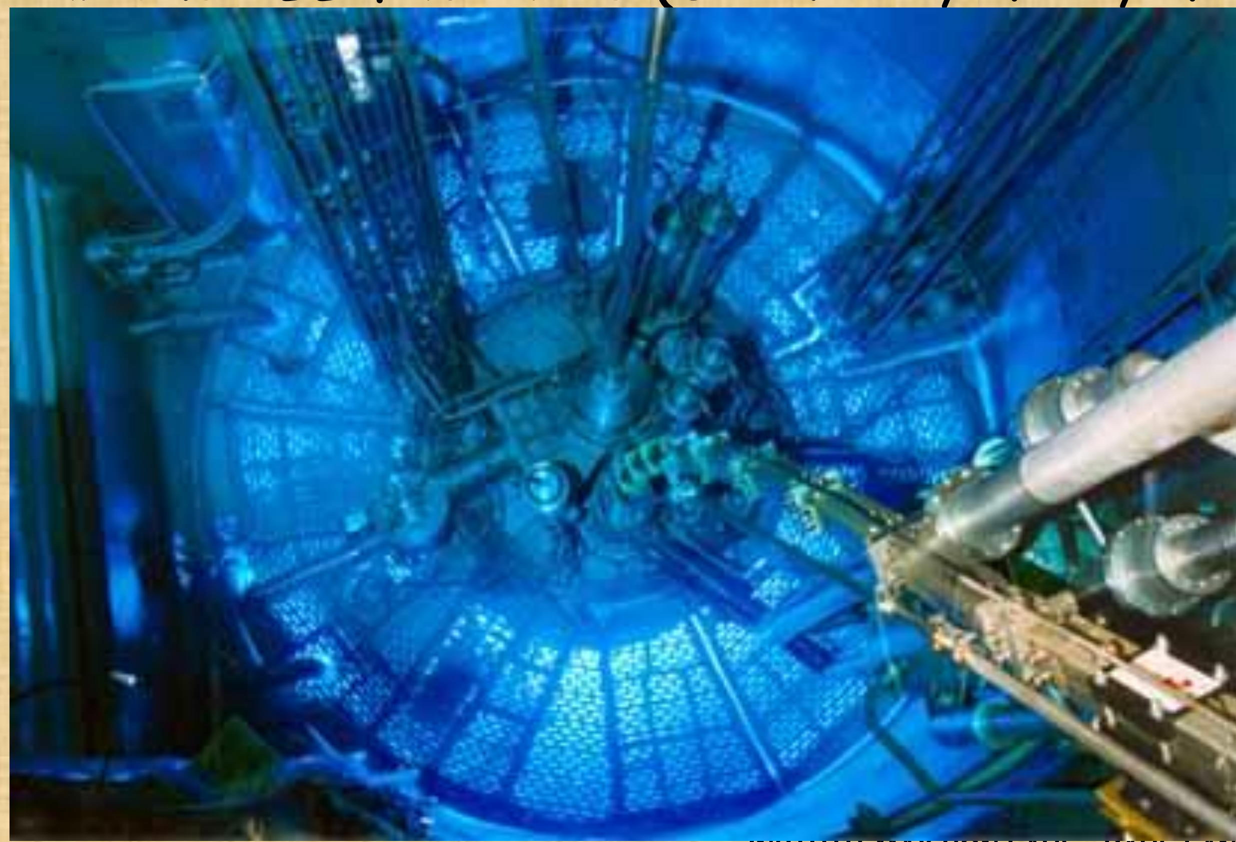

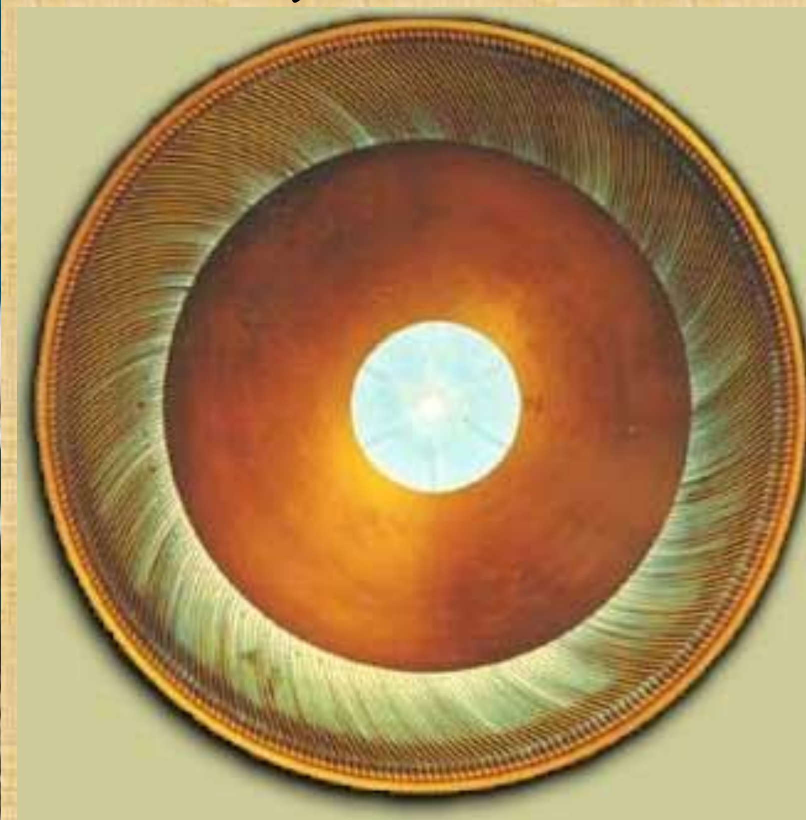

Short-range forces. State of the art.

I. Antoniadis, S. Baessler, M. Buchner, V.V. Fedorov, S. Hoedl, V.V. N., G. Pignol, K.V. Protasov, S. Reynaud, Yu. Sobolev, « Short-range fundamental forces », Compt. Rend. Phys. 12 (2011) 775.

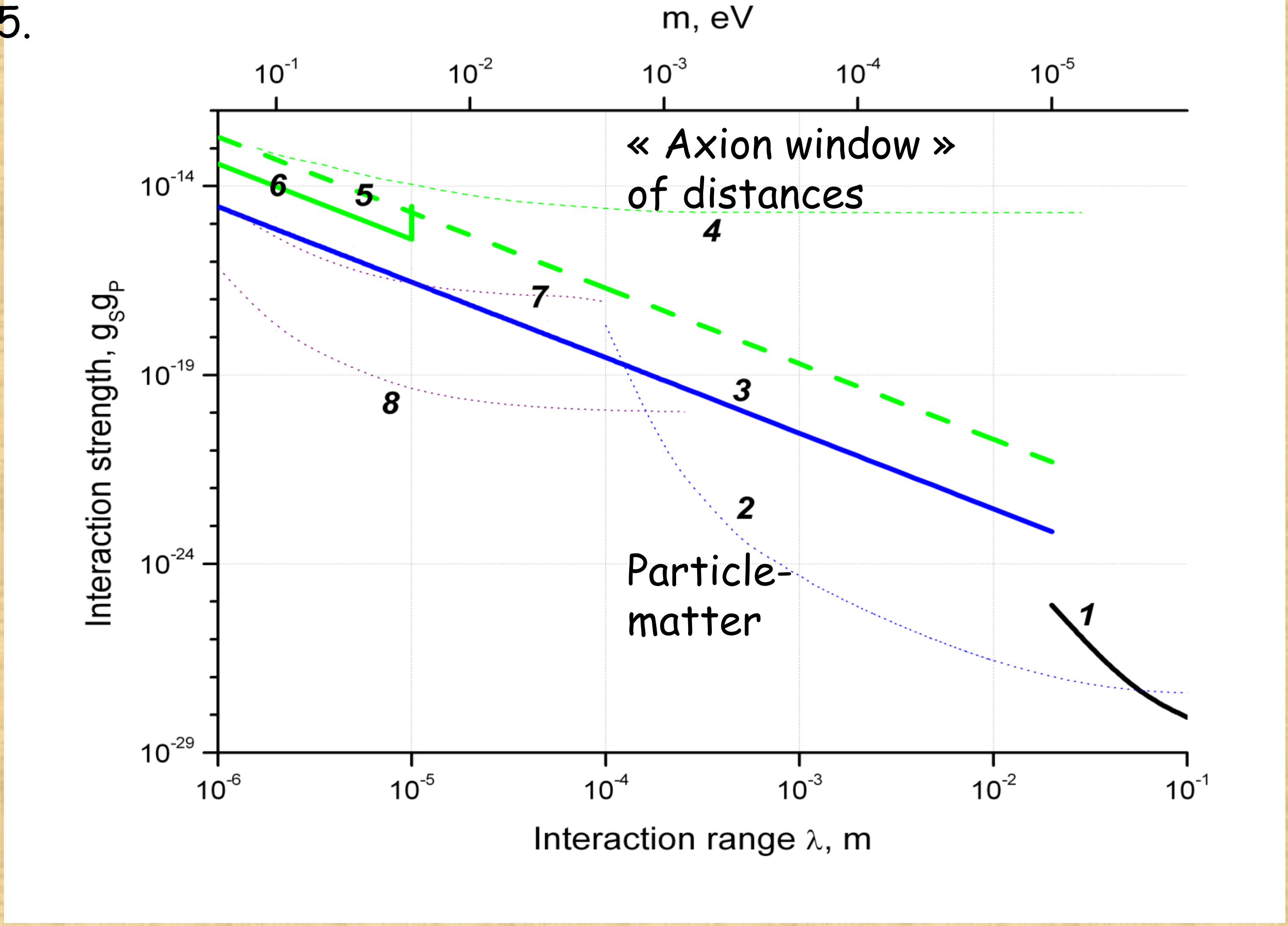

Short-range forces. More recent improvements

NEUTRONS FOR SCIENCE

Measurements using UCNs in the EDM apparatus at PSI (Villigen, Switzerland) [S. Afach et al, Phys. Let. B 745 (2015) 58].

Red line (H) shows the new constrain derived from this experiment.

Solid line (I) indicates an achievable constraint that could be obtained with a modified installation.

A slightly better (then H) constraint was measured with polarized He^3 in M. Guigue et al, Phys. Rev. D 92 (2015) 114001.

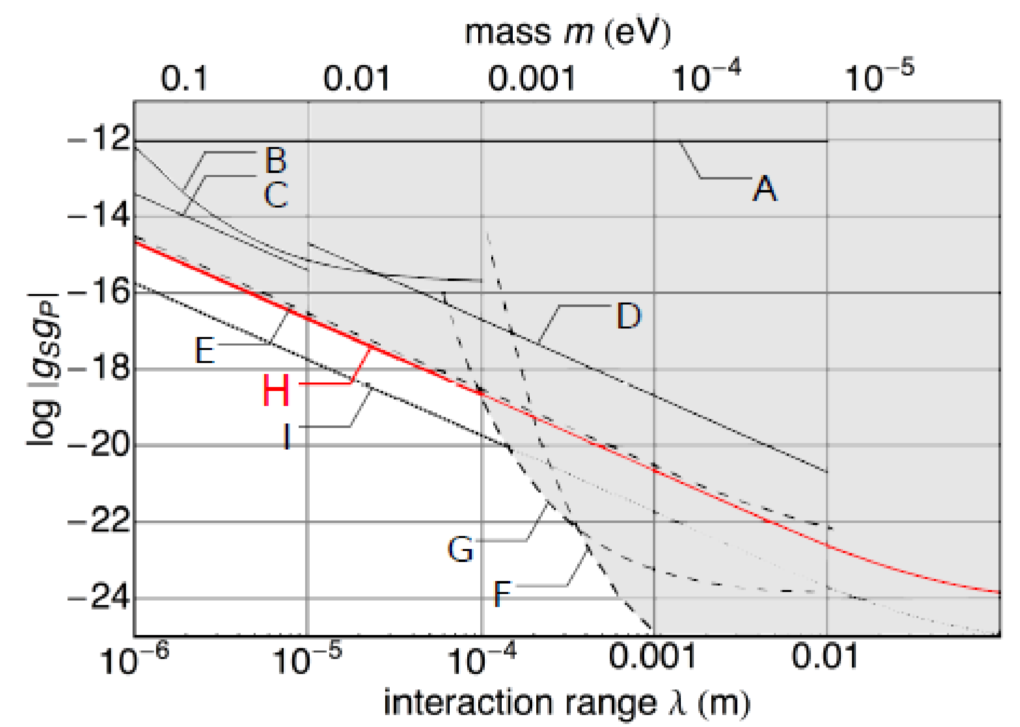

Figure 2: Overview of current limits on the product of scalar and pseudoscalar coupling constants $g_S g_P$ as function of the interaction range λ of a short range spin-dependent force at 95 % confidence level. On the top, the corresponding mass range of the mediating particle, i.e. axion or axion-like particle, is shown. The shaded region is excluded by different experiments. Solid line limits were obtained using cold or ultracold neutrons. Dashed line limits were obtained using ^{3}He, ^{129}Xe, or ^{131}Xe precession experiments. A [24]; B [25], assuming an attractive interaction; C [26]; D [6]; E [23]; F [20]; G [21]; and H (red) this work. The line I (dotted) depicts the achievable limit by a simple modification of our apparatus (see text).

Short-range forces. More recent improvements

Measurements using UCNs in the EDM apparatus at PSI (Villigen, Switzerland) [S. Afach et al, Phys. Let. B 745 (2015) 58].

Red line (H) shows the new constrain derived from this experiment.

Solid line (I) indicates an achievable constraint that could be obtained with a modified installation.

A slightly better (then H) constraint was measured with polarized He^3 in M. Guigue et al, Phys. Rev. D 92 (2015) 114001.

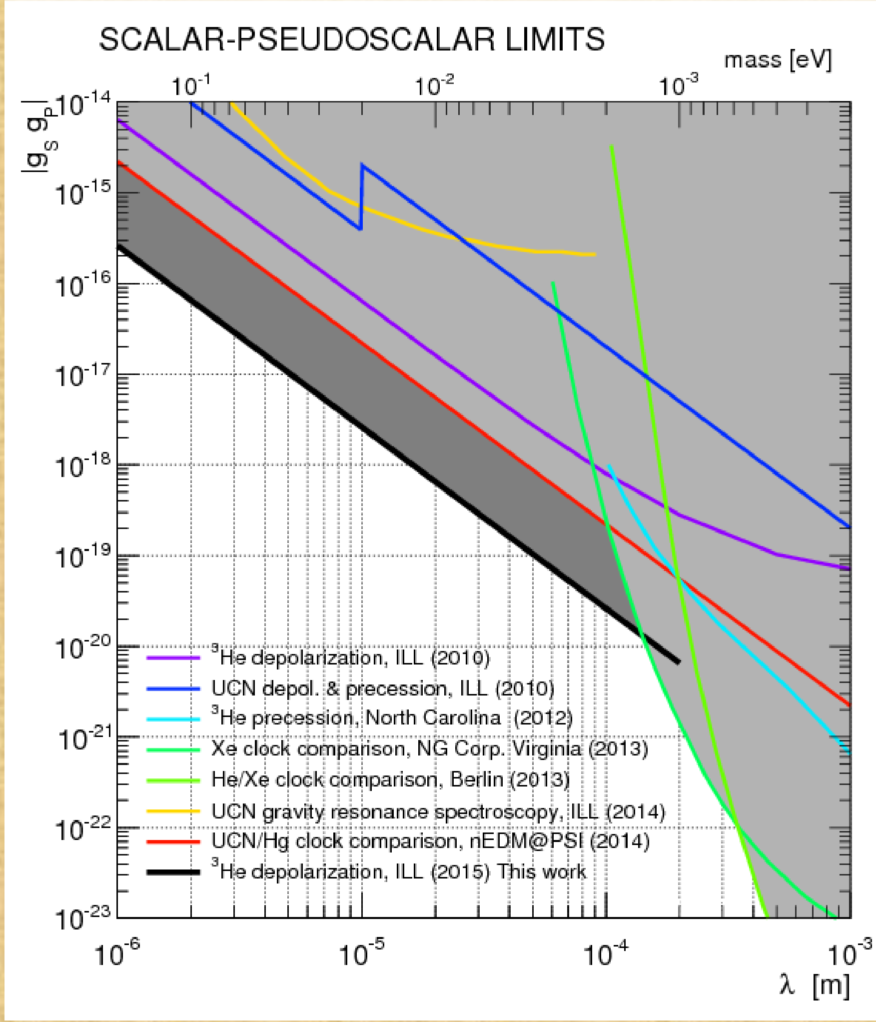

Short-range forces. State of the art.

I. Antoniadis, S. Baessler, M. Buchner, V.V. Fedorov, S. Hoedl, V.V. N., G. Pignol, K.V. Protasov, S. Reynaud, Yu. Sobolev, « Short-range fundamental forces », Compt. Rend. Phys. 12 (2011) 775.

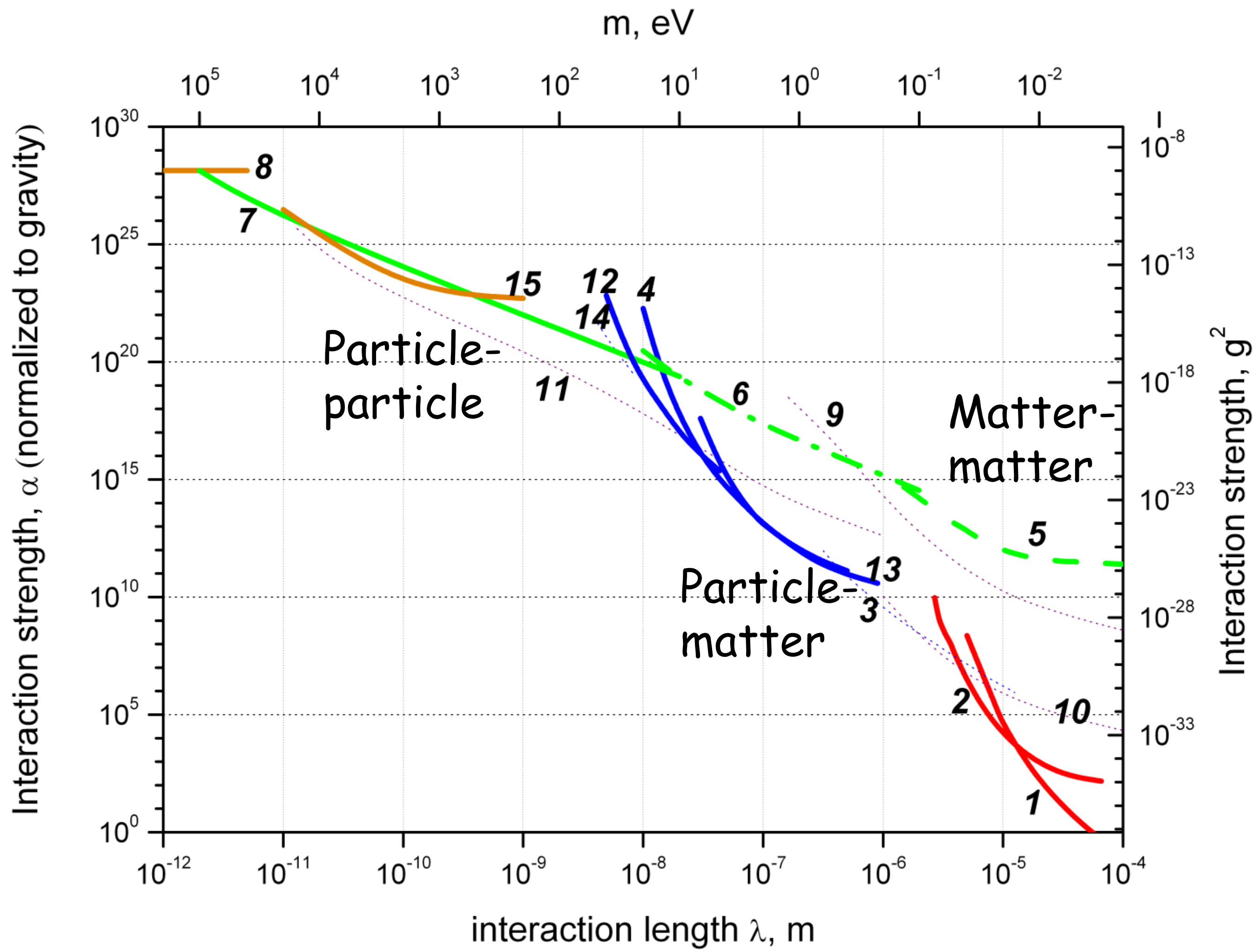

Short-range forces. State of the art.

Y. Kamiya, K. Itagaki, M. Tani, G.N. Kim, and S. Komamiya, "Constraints on new gravitylike forces in the nanometer range", ArXiv:hep-ex/1504.02181

More measurements to be done at ILL within next few years

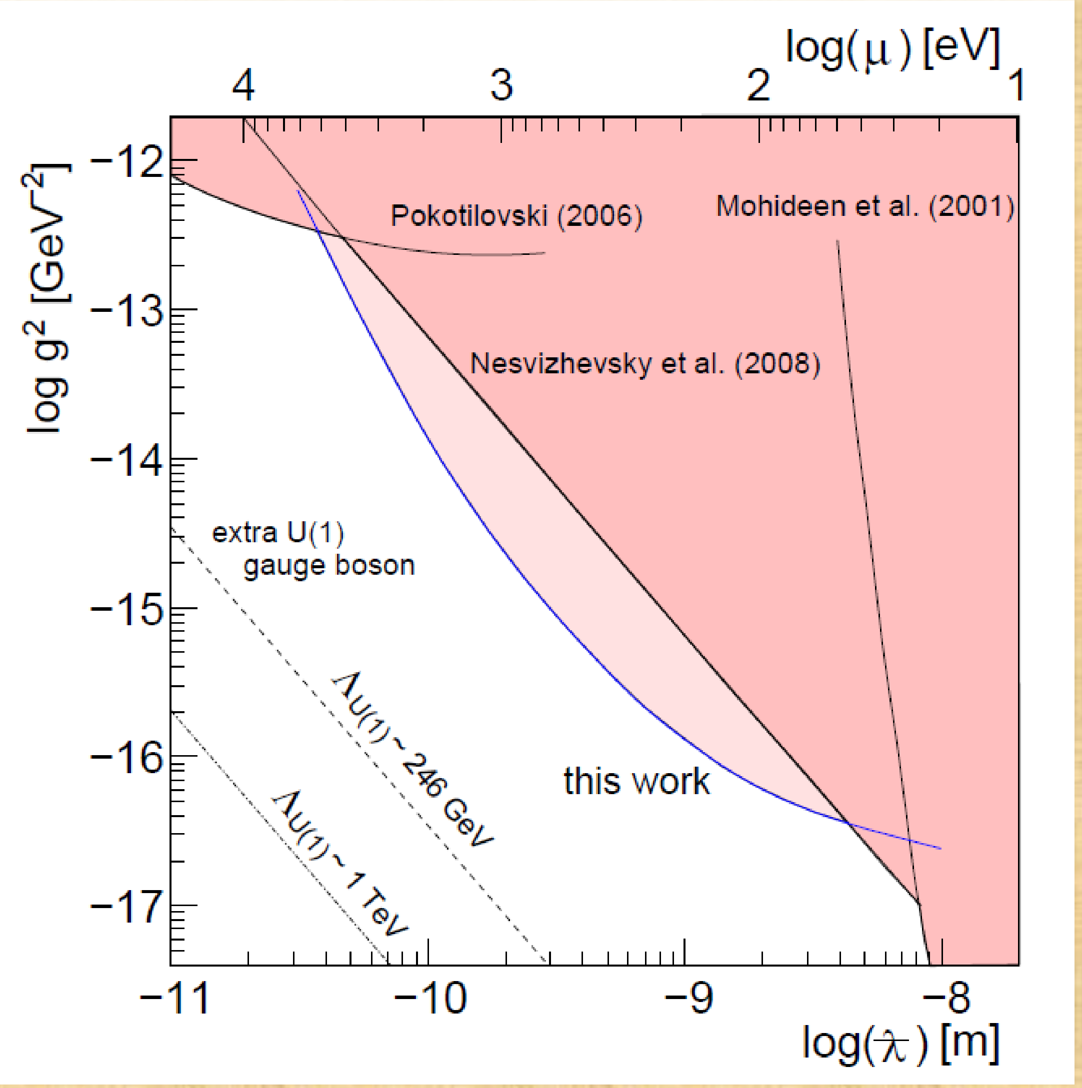

Short-range forces. More recent improvements

Neutron gravitational states.

- Several independent groups (Tokyo, QBounce, GRANIT);
- Building a dedicated facility at ILL for experiments with gravitational quantum states of neutrons in the long-storage mode (GRANIT);
- Neutron results for short-range forces are not yet competitive to results of short-range gravity and Casimir experiments but they are rapidly improving (remember that one should improve by 5-6 orders of magnitude; however, no major systematic effects associated with neutrons have been identifies);
- Significant worldwide effort to increase available densities of UCNs.

Transitions between gravitational quantum states

Flow-through mode; limited observation time

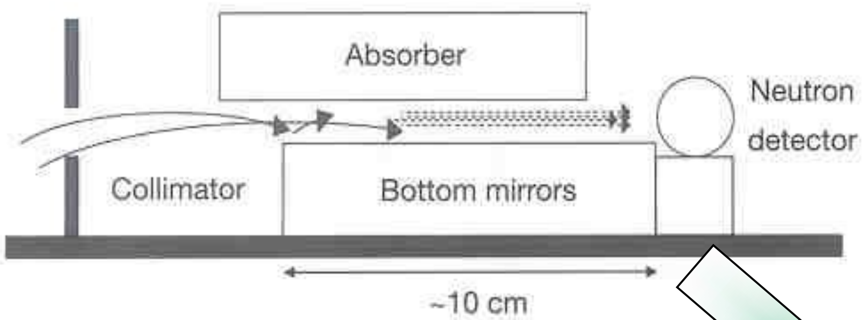

Figure 2 Layout of the experiment. The limitation of the vertical velocity co... depends on the relative position of the absorber and mirror. To limit the horizonta... component we use an additional entry collimator. The relative height and size of the e... collimator can be adjusted.

Transitions could be excited, for instance:

- By periodically varying magnetic field gradient;

-By periodically varying local gravitational field;

-By oscillating mechanically the mirror.

V.V. N., and K.V Protasov, "Quantum states of neutrons in the Earth's gravitational field: state of the art, applications, perspectives" in Edited book on Trends in Quantum Gravity Research (D.C. Moore, New York, USA, NOVA, 2005; pp. 65-107)

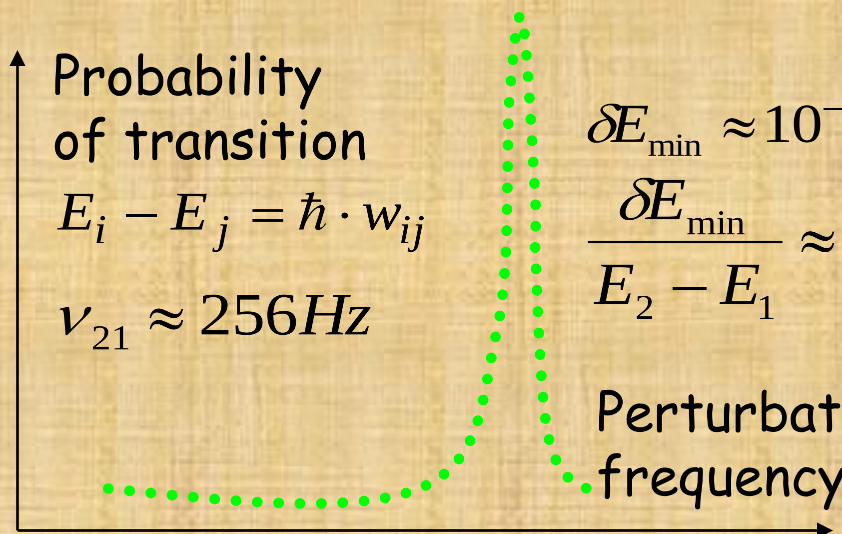

$$E_i - E_j = \hbar \cdot w_{ij}$$

$$\nu_{21} \approx 256 Hz$$

$$\delta E_{\min} \approx 10^{-18} eV$$

$$\frac{\delta E_{\min}}{E_2 - E_1} \approx 10^{-6}$$

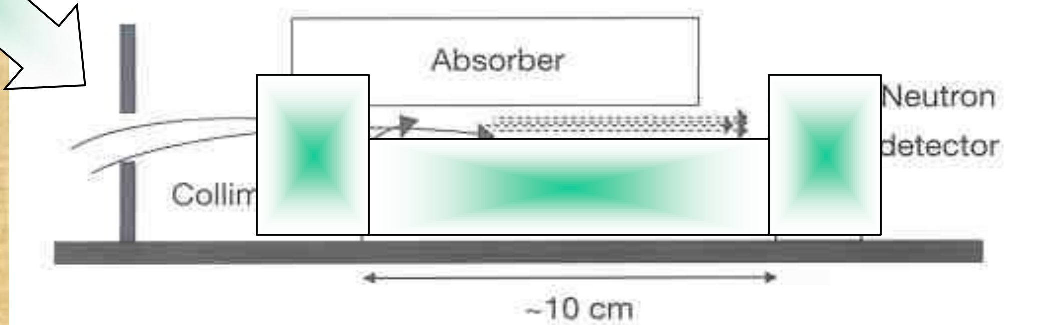

Storage mode: ultimate observation time and energy resolution

Gravitational quantum states in a storage mode

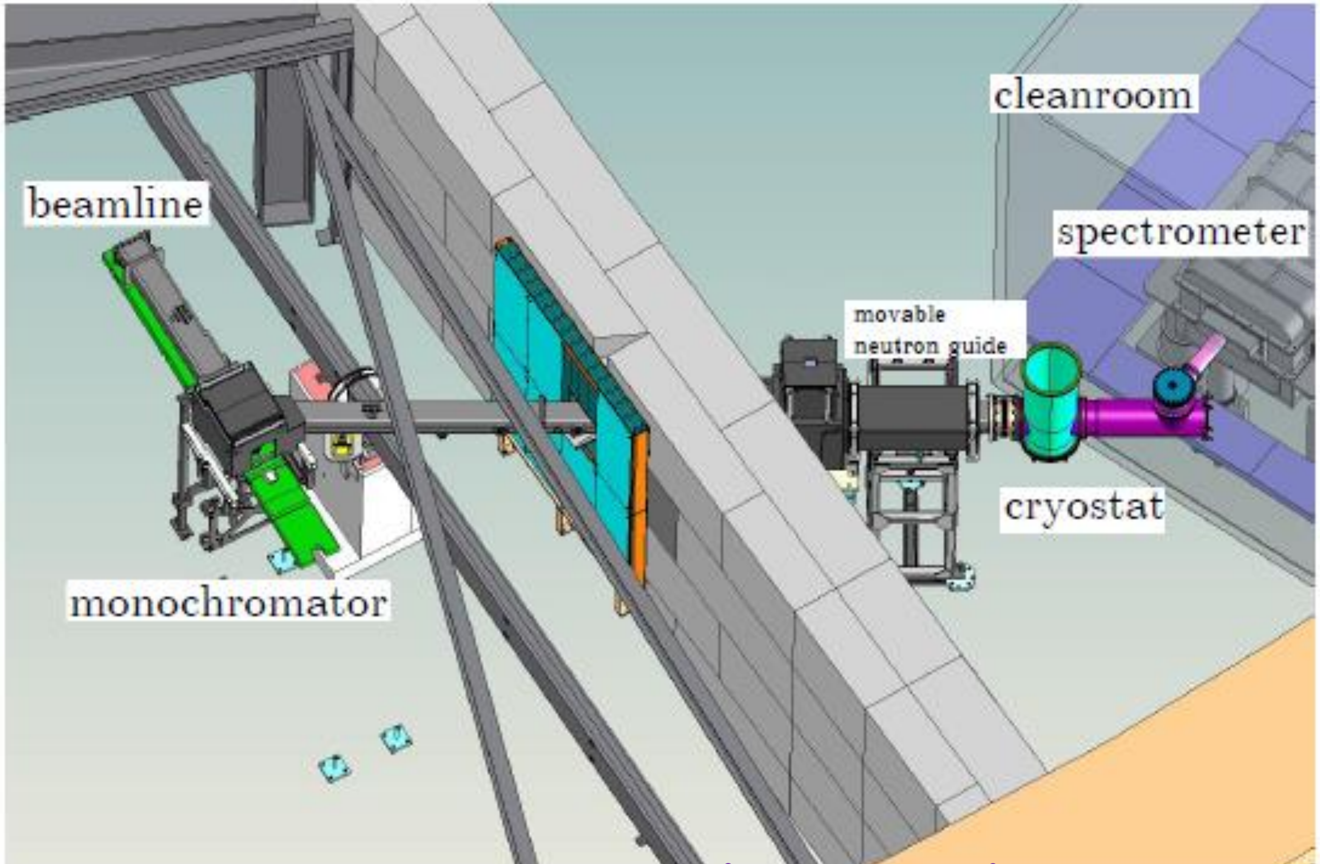

Mirrors are similar to those in the gravitational wave detectors

FIG. 1: The GRANIT instrument at Level C of ILL, Grenoble.

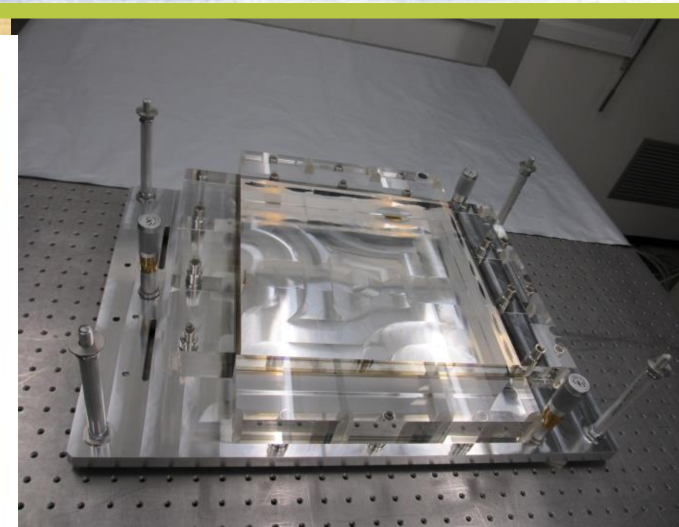

Granit
Gravitational Neutron Induced Transitions

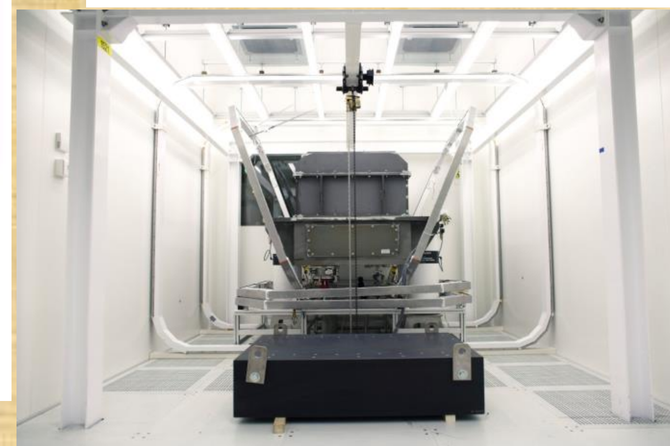

Gravitational quantum states in a storage mode

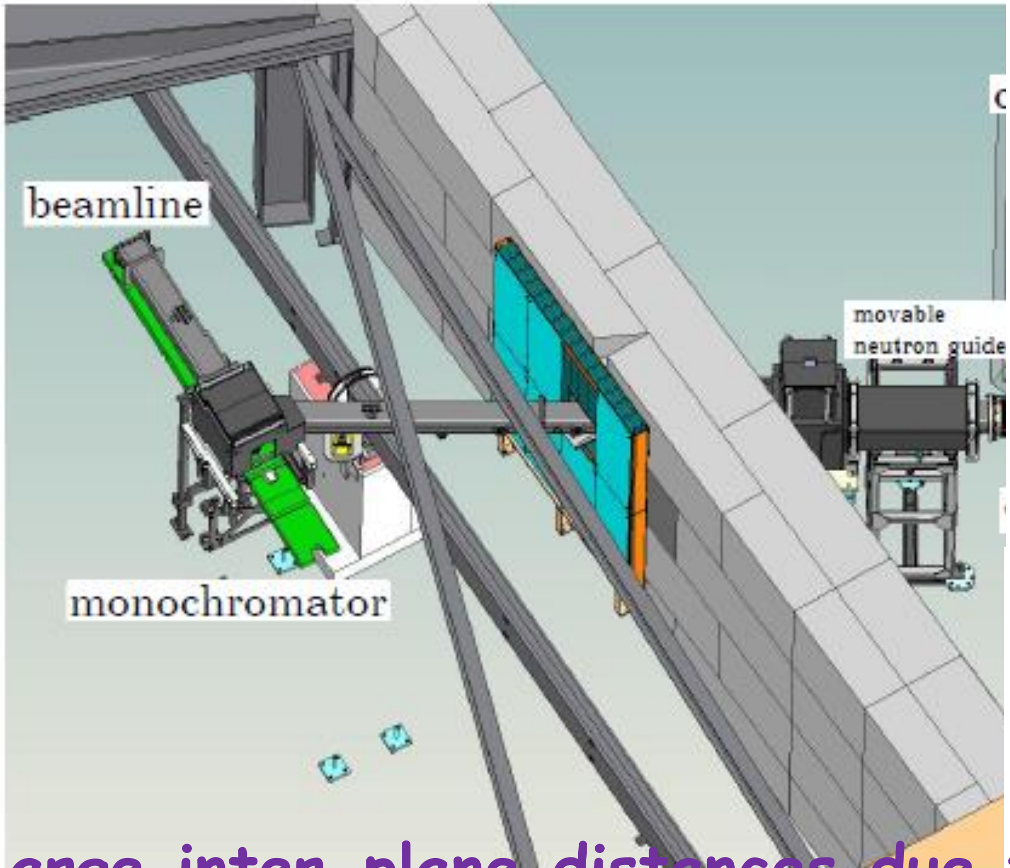

Large inter-plane distances due to intercalated graphite technology

FIG. 1: The GRANIT instrument at Level C o
ble.

Precision characterization of the resulting neutron beam

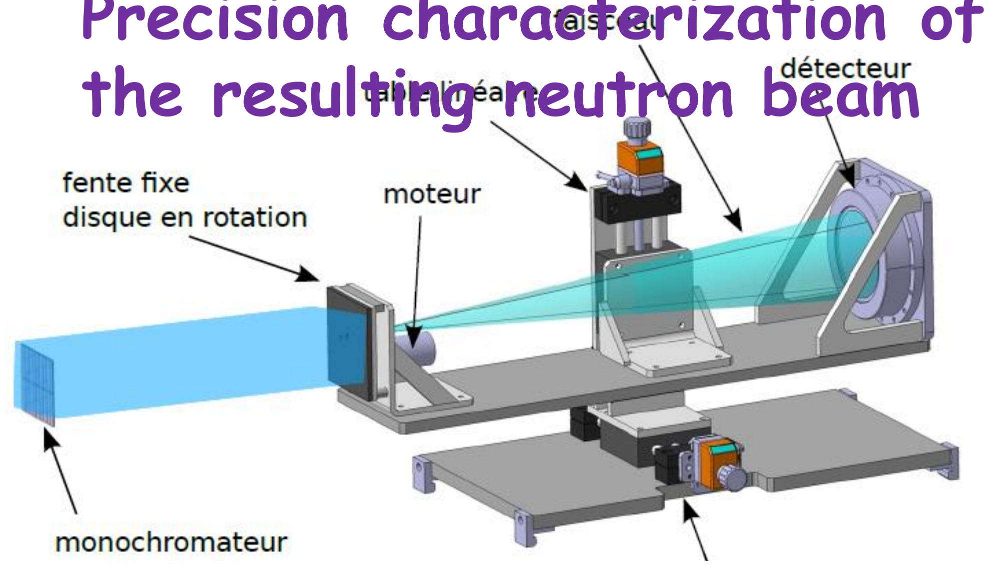

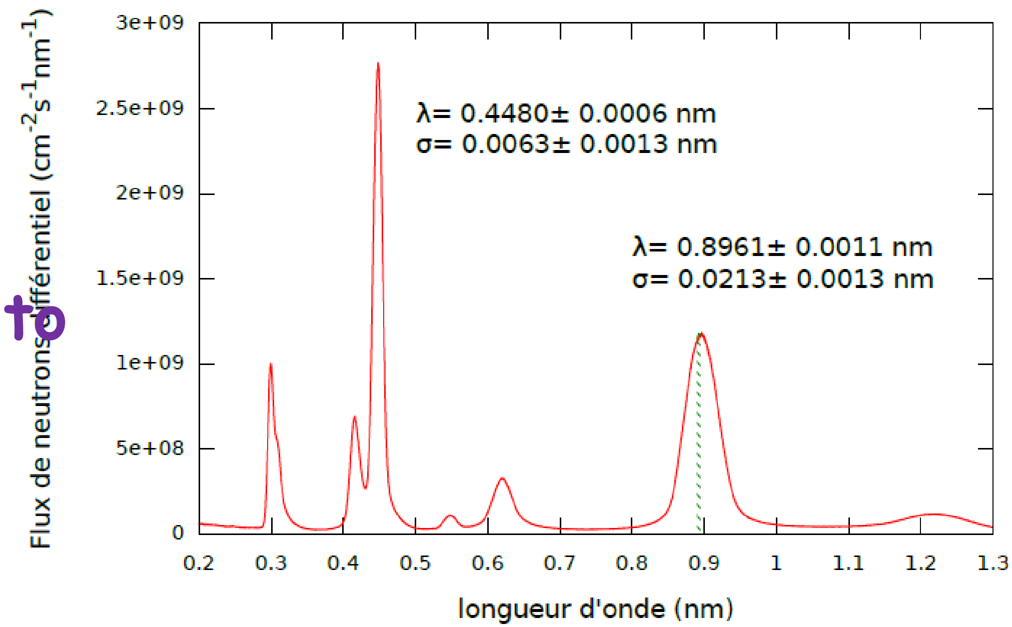

Gravitational quantum states in a storage mode

NEUTRONS FOR SCIENCE

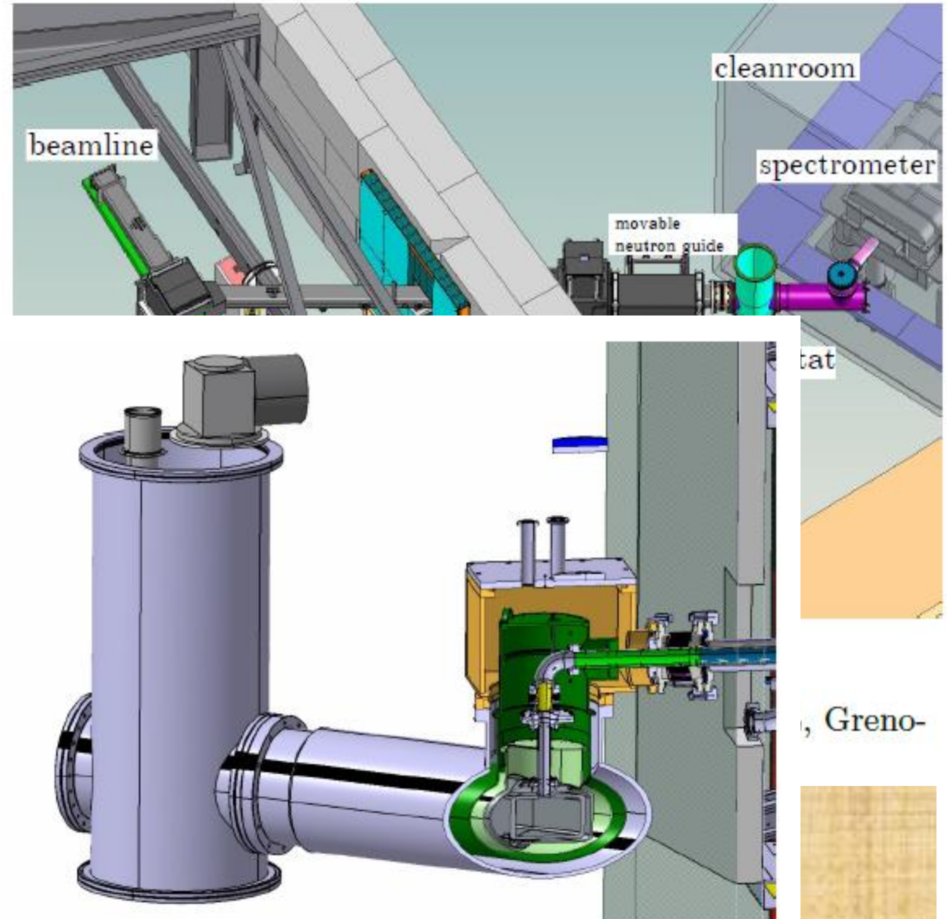

FIG. 6: Extraction guides from the source to the spectrometer. The extraction guides are composed of several tubular elements, which are thin foils of stainless steel inserted inside tubes. The design of the guides allows compensating for the misalignment between the source and the spectrometer.

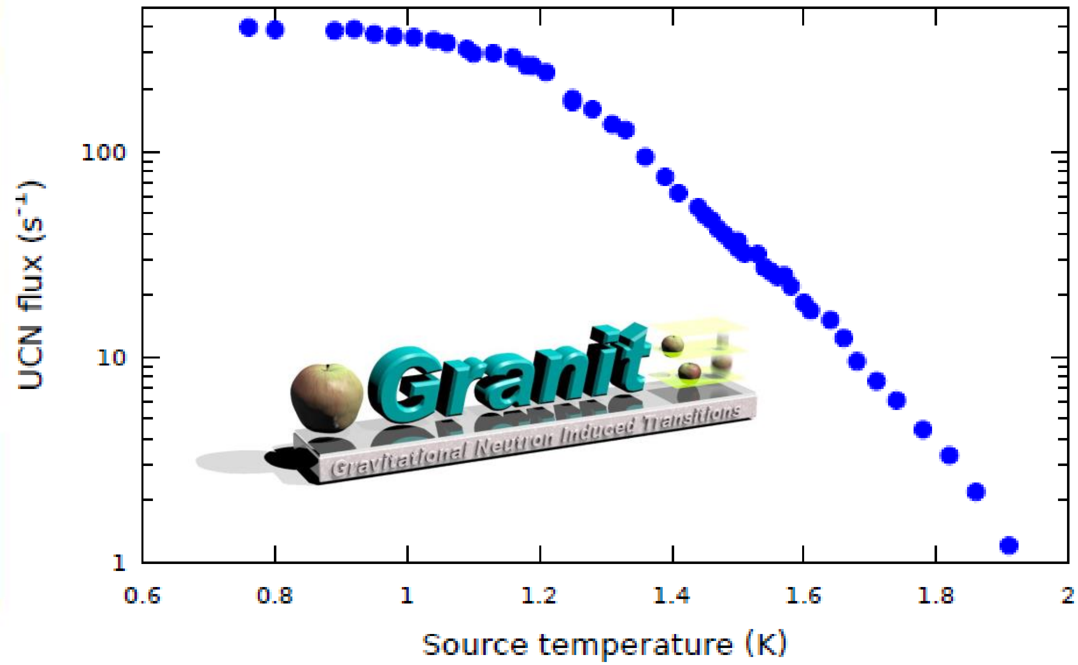

FIG. 10: UCN countrate versus the temperature of He-II The cold neutron beam constantly passes through the source and the UCN valve is opened periodically.

The first He-4 UCN source providing UCNs for a "user" experiment (record brightness, small volume)

NEUTRONS
FOR SCIENCE

GRANIT first measurements

- The simplest configuration of the GRANIT spectrometer in the flow-through mode is similar to the first observation of gravitational quantum states;
- Neighbouring quantum states have never been clearly resolved experimentally;
- This is needed for 1) measuring much more precisely the parameters of quantum states, 2) for providing contrast in experiments with resonance transitions between gravitational quantum states.

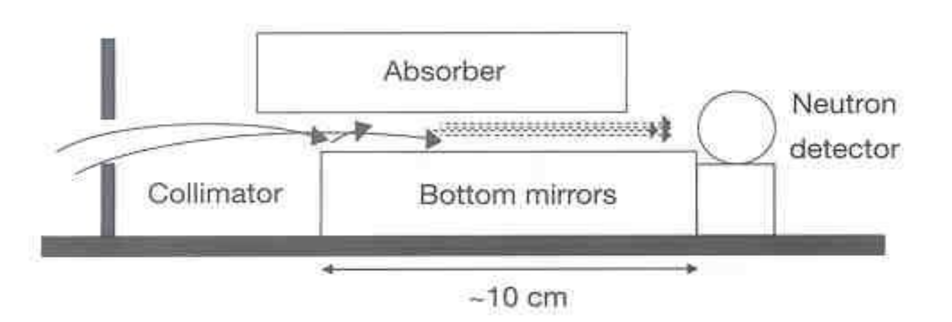

Figure 2 Layout of the experiment. The limitation of the vertical velocity component depends on the relative position of the absorber and mirror. To limit the horizontal velocity component we use an additional entry collimator. The relative height and size of the entry collimator can be adjusted.

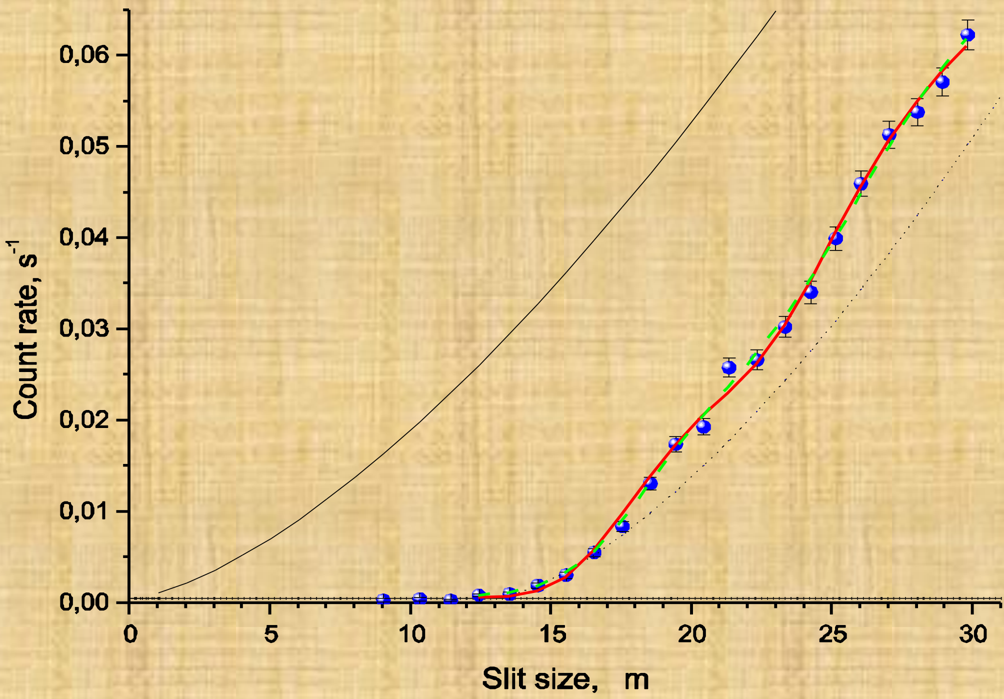

GRANIT first measurements

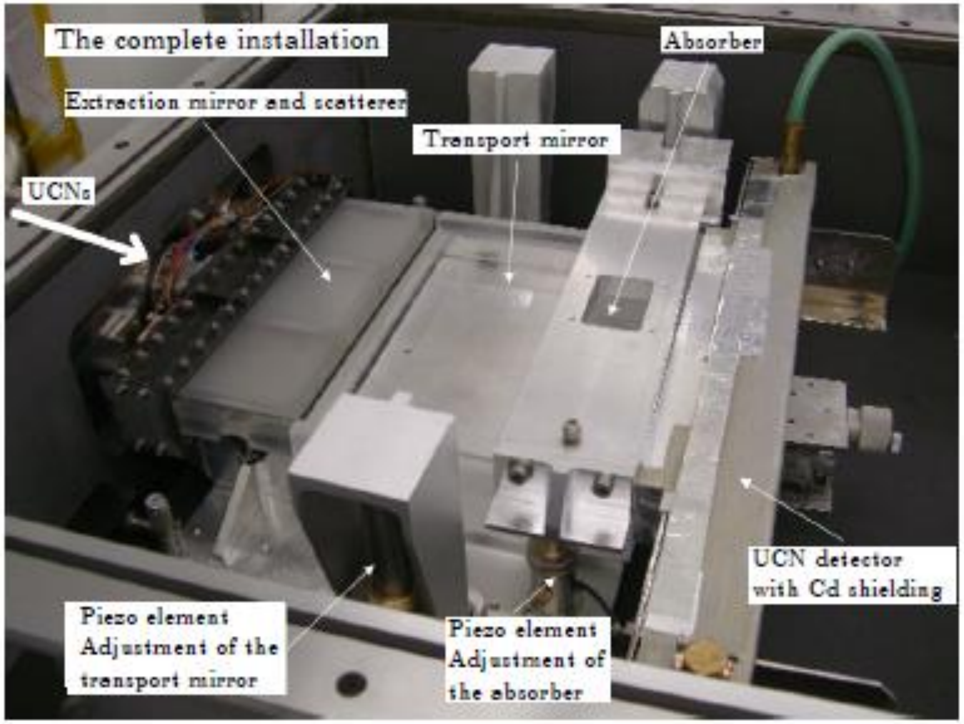

FIG. 17: The optical elements on the granit table. The extraction mirrors assembly and the transport mirror are placed on two separate adjustable supports. Their adjustment could be done with 3 + 3 micrometric screws. To adjust the height and the orientation of the surface of the transport mirror with a great accuracy, we use 3 piezo-electric elements. The distance between the absorber and the transport mirror is adjustable as well using 3 piezo-electric elements. The piezos are driven from the control computer with a Labview application.

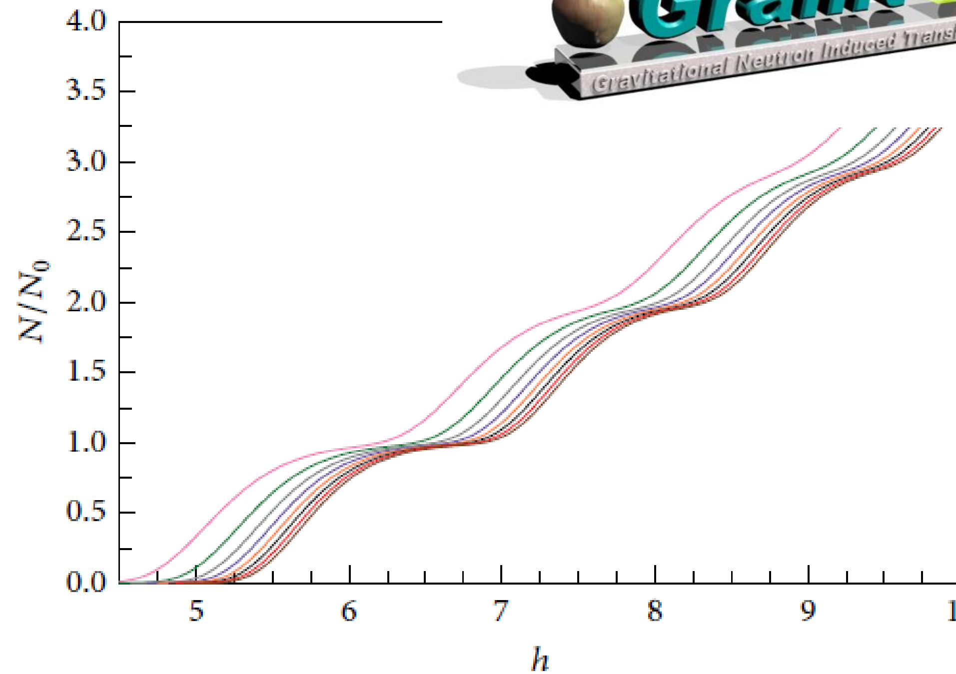

FIGURE 4: The exit neutron count N_e/N_0 as a function of the slit width h for several values of Φ_2 close to 5×10^3 (N_0 is the number of neutrons entering the slit in each quantum state). Eight curves from left to right correspond to $\Phi_2 \times 10^{-3} = 1; 2; 3; 4; 5; 6; 7; 8$; neutron count decreases with increasing Φ_2.

First result are **promising!** 1) the absorber is more **efficient** by an order of magnitude, 2) UCN flux is **sufficient**, 3) backgrounds are **acceptable**.

GRANIT first measurements

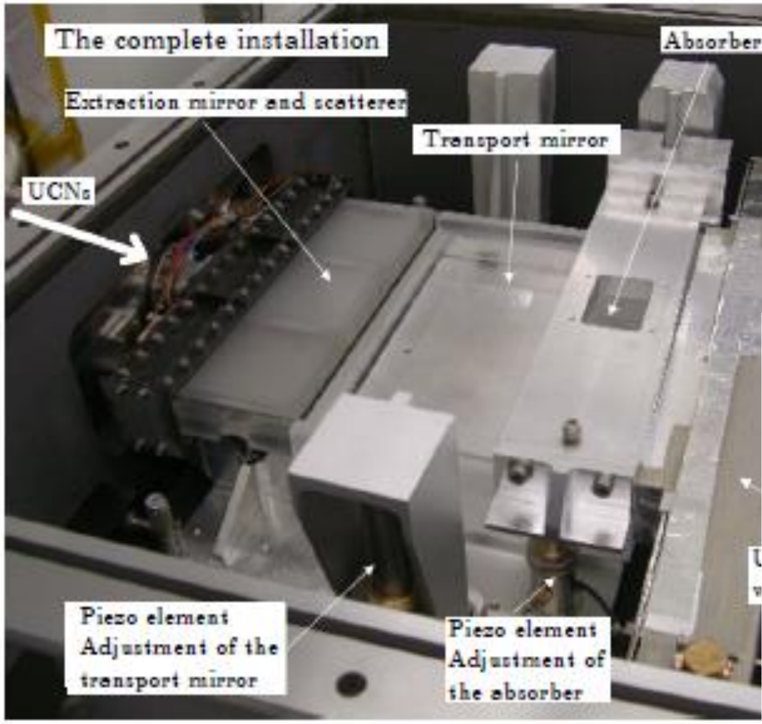

FIG. 17: The optical elements on the granit tab
traction mirrors assembly and the transport mirro
on two separate adjustable supports. Their adjus
be done with 3 + 3 micrometric screws. To adjus
and the orientation of the surface of the transport
a great accuracy, we use 3 piezo-electric element
tance between the absorber and the transport m
justable as well using 3 piezo-electric elements. Th
driven from the control computer with a Labview

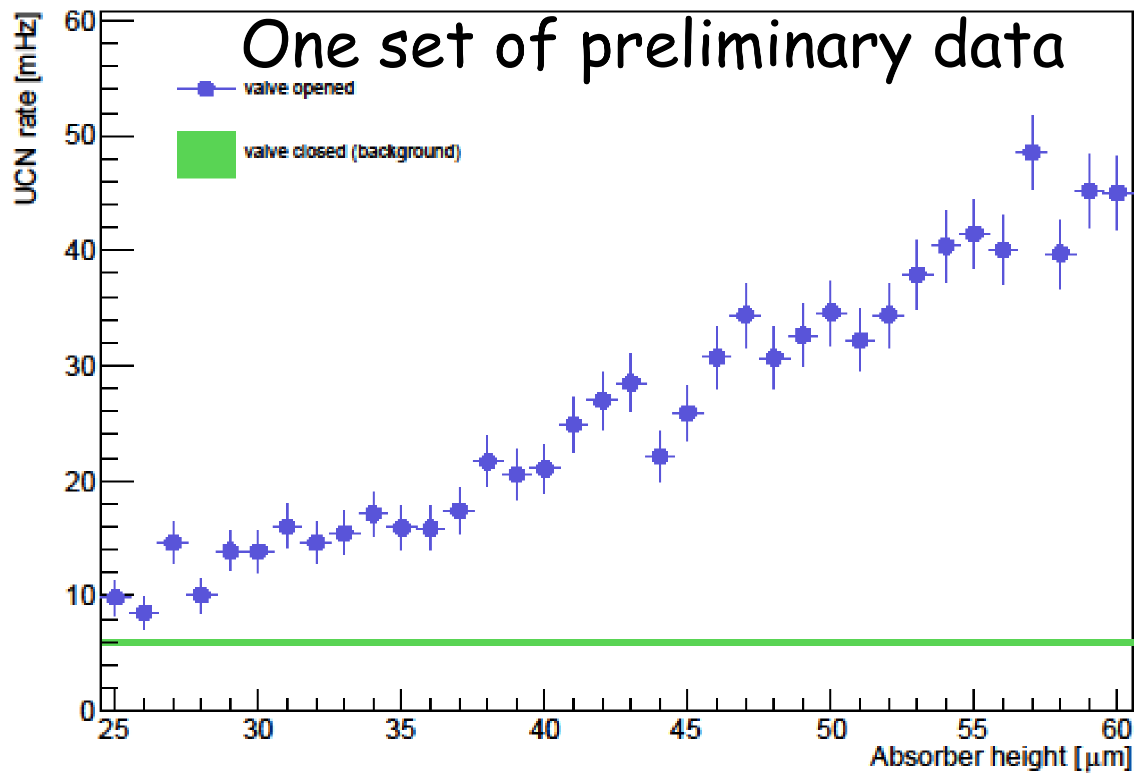

Real-time position-sensitive UCN detectors of high resolution (by Benoit Clement et al)

B10 converters

$n + {}^{10}B \rightarrow {}^{7}Li + \alpha$, BR = 6.3%

E_{Li}= 1014 keV E_{α} = 1775 keV

$n + {}^{10}B \rightarrow {}^{7}Li^{*} + \alpha \rightarrow {}^{7}Li + \alpha + \gamma$, BR = 93.7%

E_{Li}= 841 keV E_{α} = 1471 keV E_{γ}= 478 keV

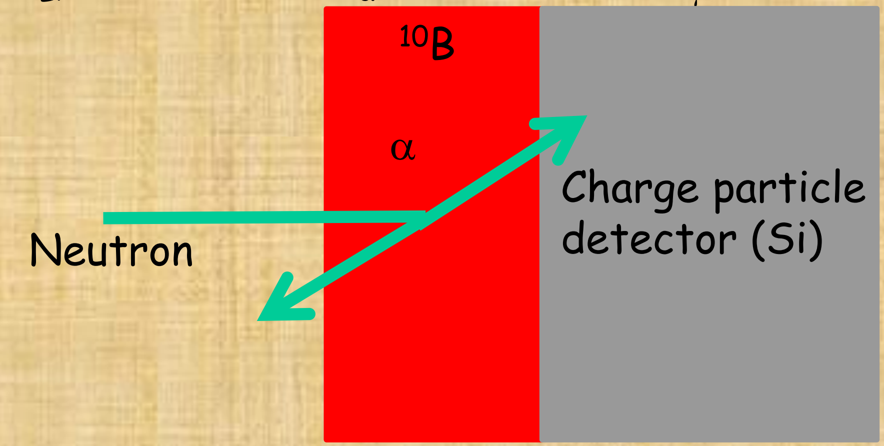

The conversion layer must be
- thick enough to absorb UCNs
- thin enough to allow α/Li to escape

Thin layer deposition of B10

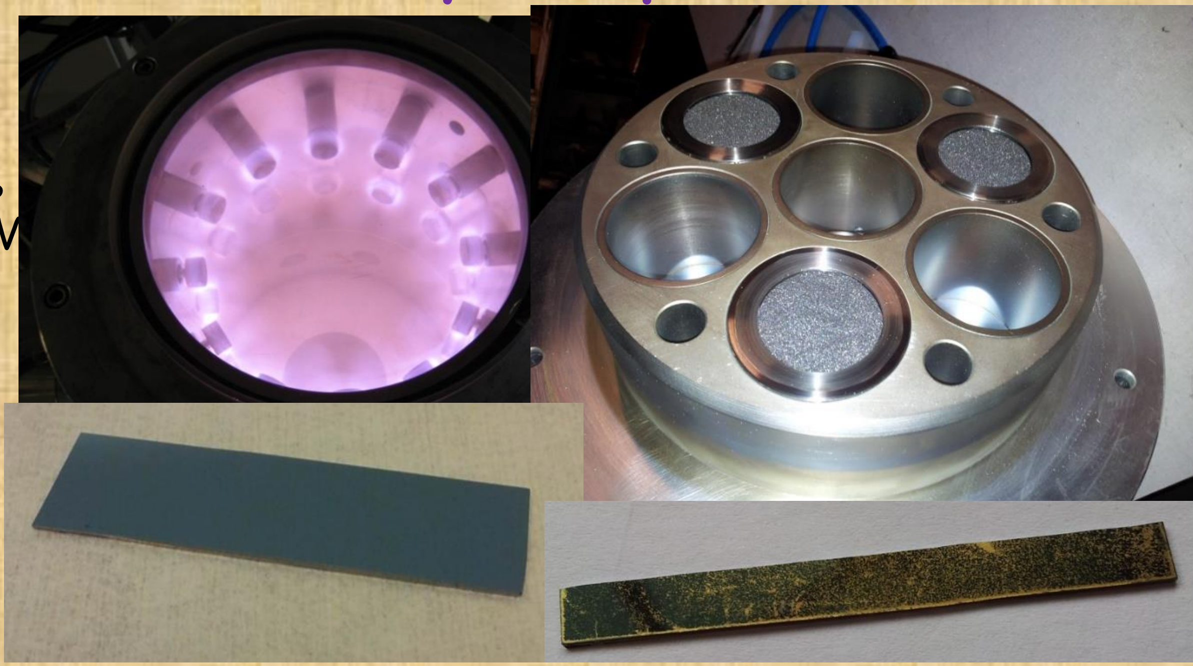

Process developped at LPSC using plasma PVD
- 200 nm B layers
- intermediate layer : Ni (~20 nm)
- surface layer : 15-20 nm Ti

Position-sensitive UCN detectors of high resolution

The role of Ti and Ni layers

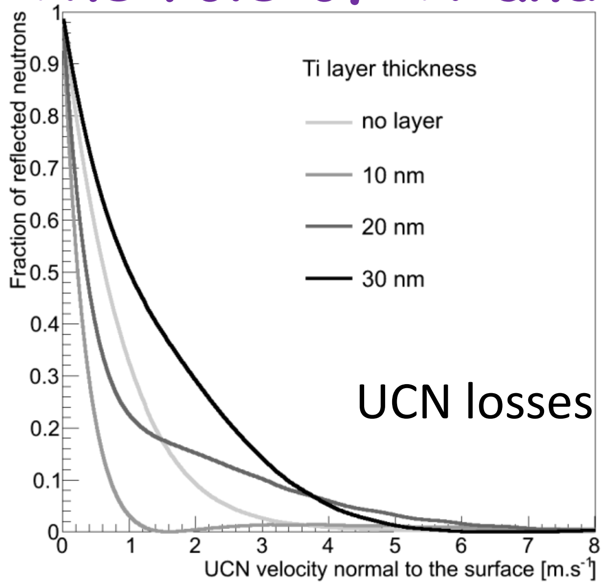

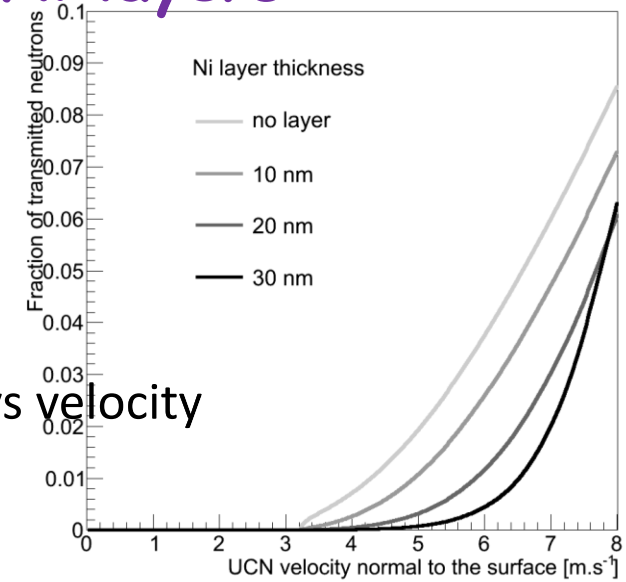

UCN losses vs velocity

The Ti layer reduces the reflection of slow UCNs, if thin enough;

The Ni layer reflects faster UCNs passing through the **B10** layer

The efficiency

20 nm entrance Ti layer; 20 nm back Ni layer; account for energy losses in the layer(s); a few 100 keV detection threshold; 200nm ^{10}B 84% to 88% efficiency, almost independent of UCN velocity

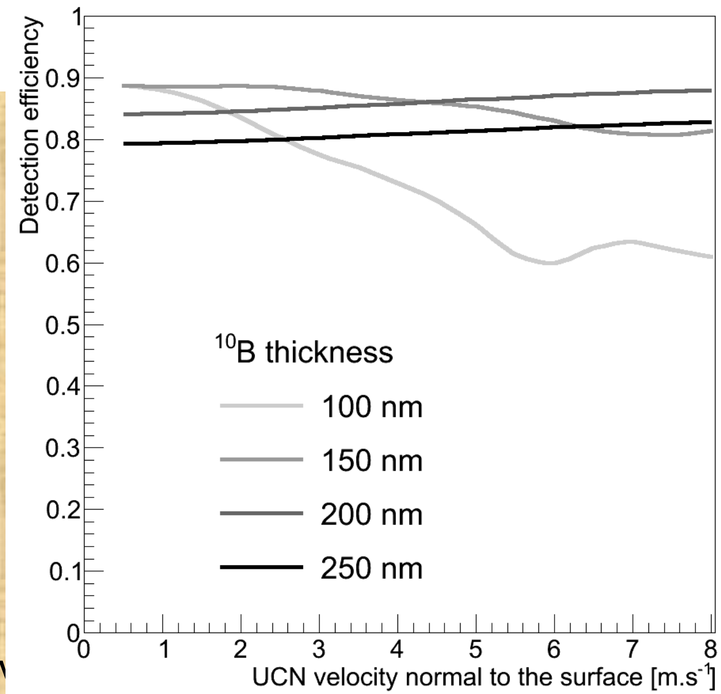

Position-sensitive UCN detectors of high resolution Resolution

UCN Boron piXels : pixelized detector using commercial CCD sensors: Windowless CCD; Ti-B-Ni layer on top of CCD; Hamamatsu P11071-1106N; 2048x64 pixels 14x14 μm; reconstructed barycenter of alpha clusters

Estimated resolution : ~1μm

Test with UCNs

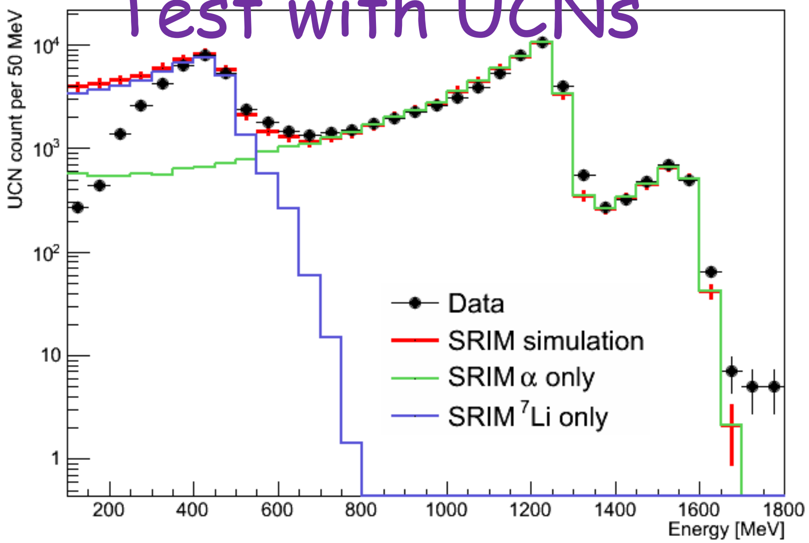

Energy measurement can be used to improve the spacial resolution for neutrons

Test with α-particles

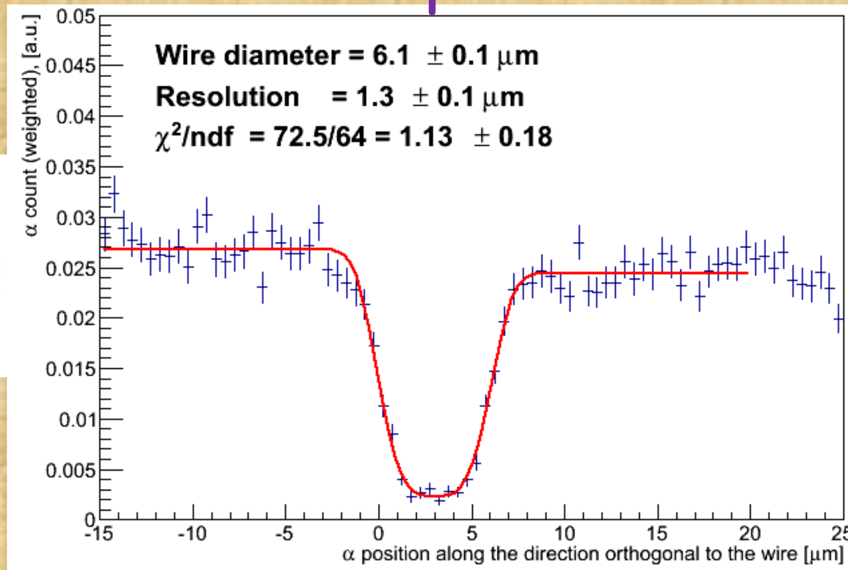

Test with cold neutrons at PF1B

The spatial resolution for neutrons is better than 3 μm as expected

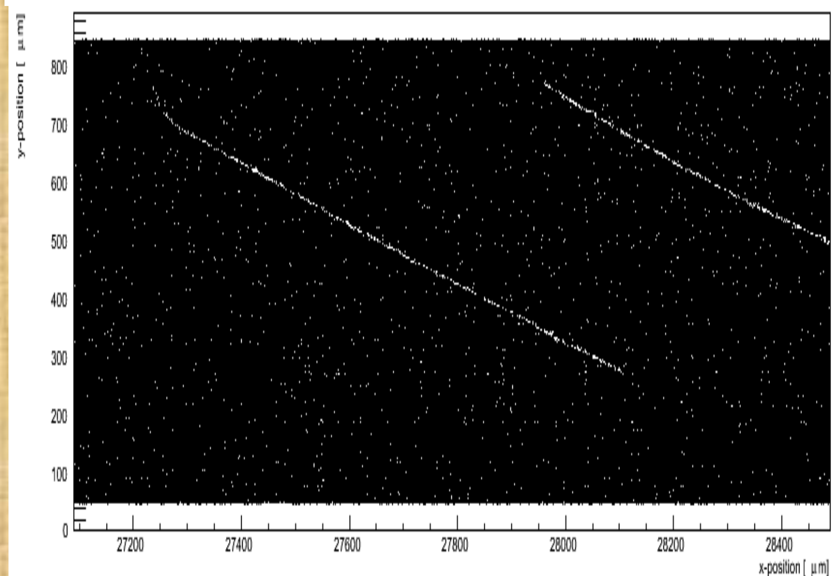

Position-sensitive UCN detectors of high resolution

UCNBox detector

8 CCD (20cm active region), vertical position and tilt adjustable, dedicated electronics

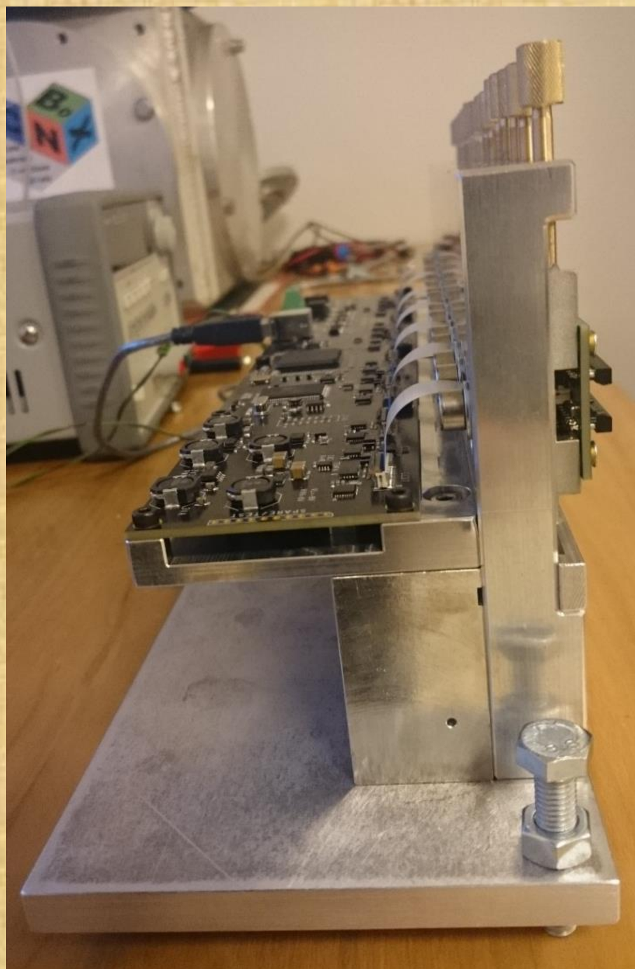

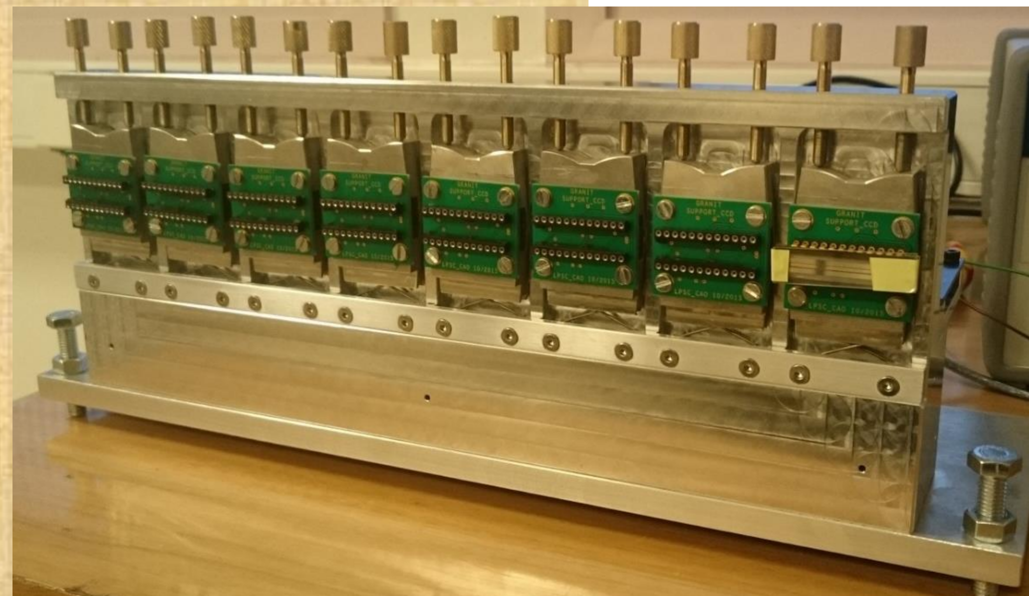

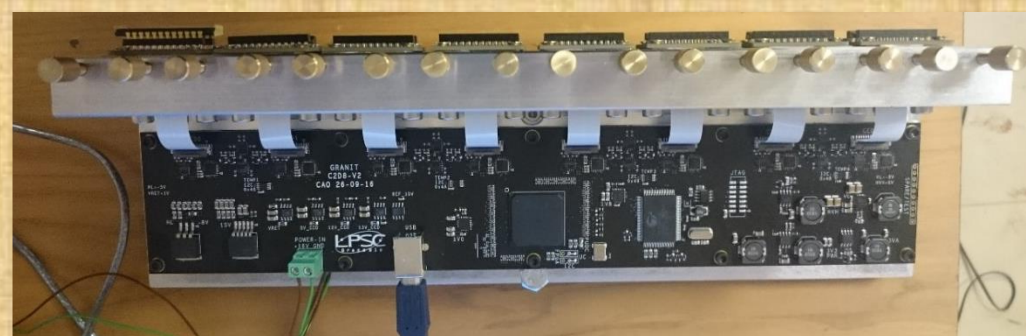

Neutron Whispering Gallery

Better precision and reliability for experiments with neutron whispering gallery; record sensitivity; good chances for major improvements

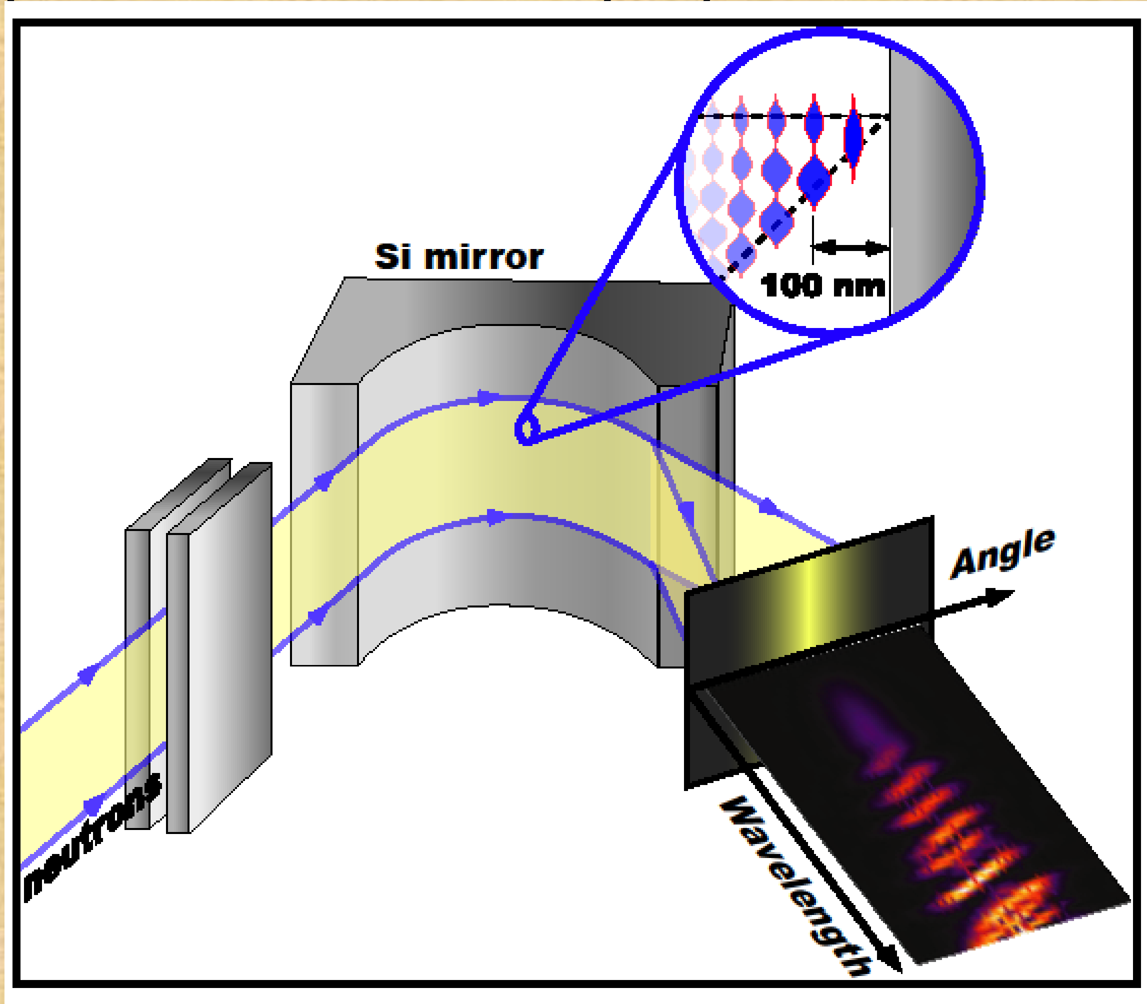

Neutron Whispering Gallery

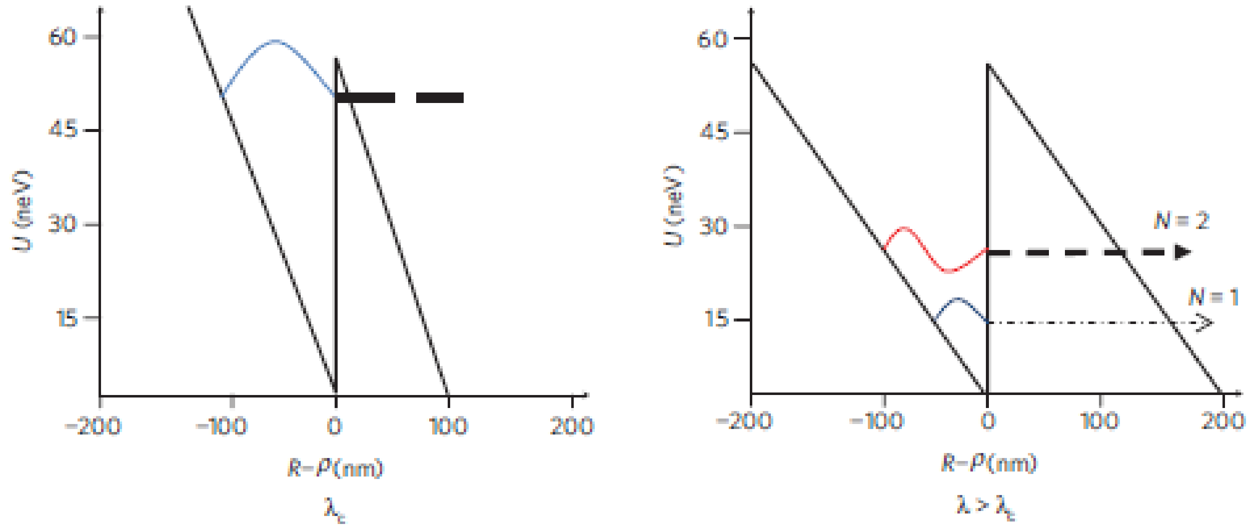

Figure 2 | A sketch of the effective potential in the cylindrical reference system. The potential step at $z = 0$ is equal to the mirror optical potential U_0. The potential slope at $z \neq 0$ is governed by the centrifugal acceleration $a_{centr} = v^2/R$. The wavefunctions of the two lowest quantum states ($n = 1,2$) are shown inside the bounding triangle potential at the height corresponding to their energies. The dashed lines illustrate tunnelling of neutrons through the bounding triangle potential.

Neutron Whispering Gallery

First observation in 2010 (experiment versus theory) with a Si concave mirror

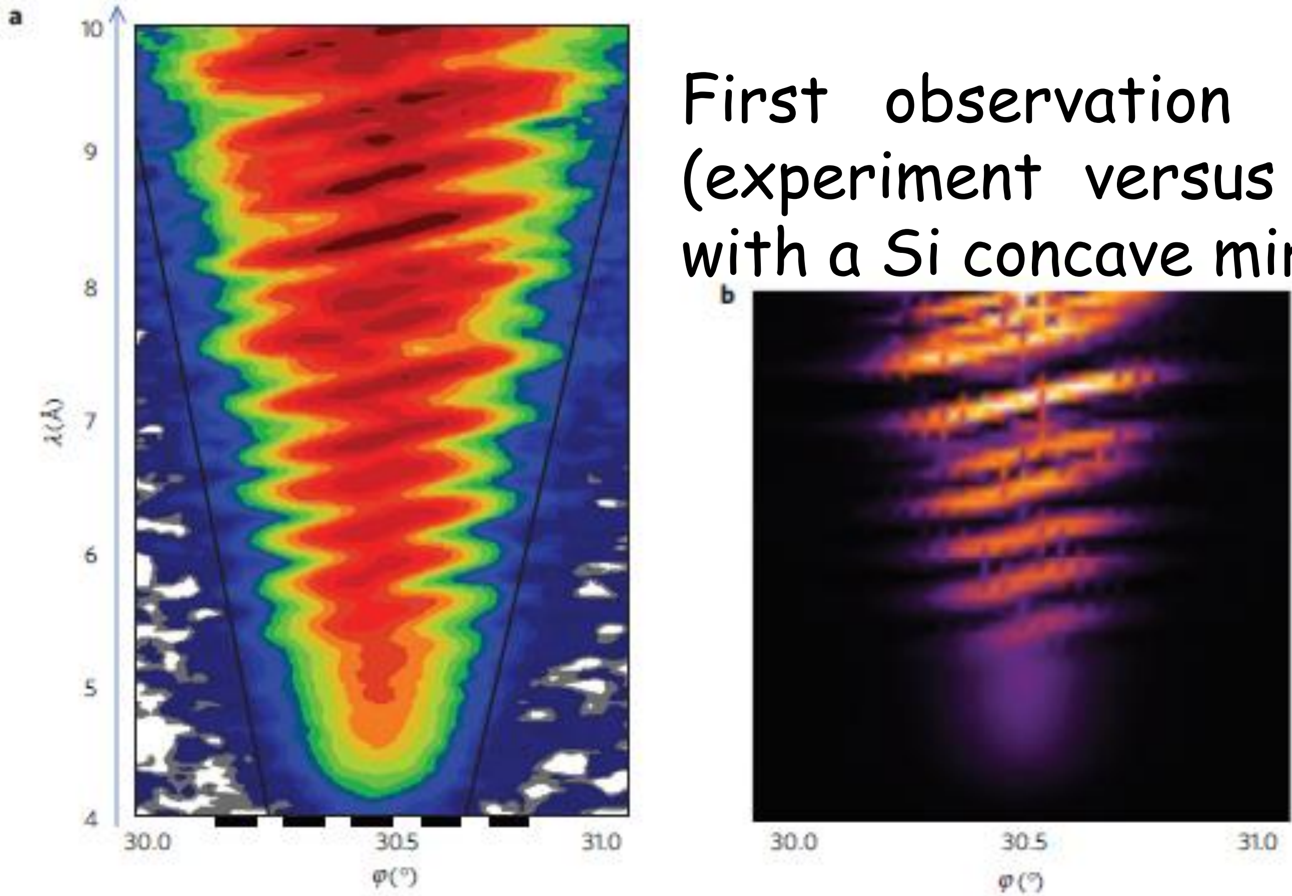

Figure 4 | Long-living centrifugal quantum states. a, The scattering probability as a function of neutron wavelength λ (Å; vertical axis) and deviation angle φ (°; horizontal axis). Neutrons enter through the entrance edge of the mirror. The geometrical angular size of the mirror is 30.5°. The inclined solid lines show the signal shape for the classical Garland trajectories. The dashed horizontal line illustrates a characteristic wavelength cutoff λ_c. **b**, Theoretical simulation of the data in accordance with refs 9–11. Some of the difference between these two pictures is probably due to the thin oxide layer on the mirror surface.

Neutron Whispering Gallery: methods

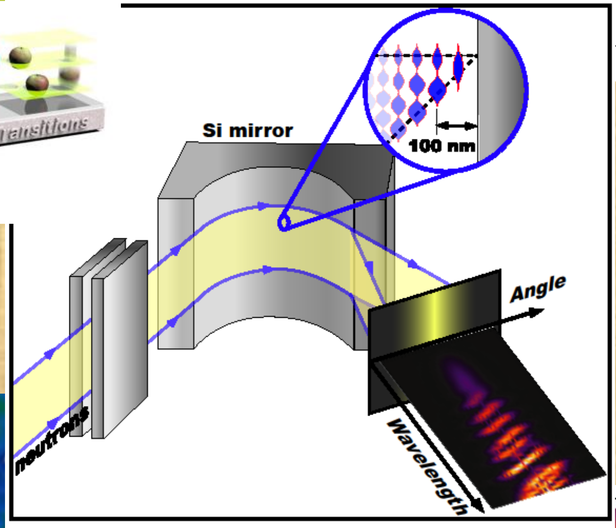

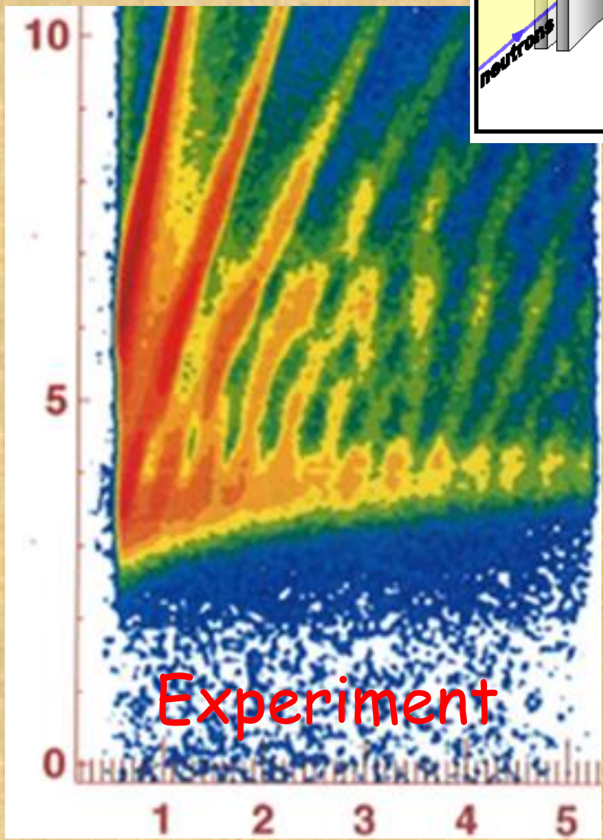

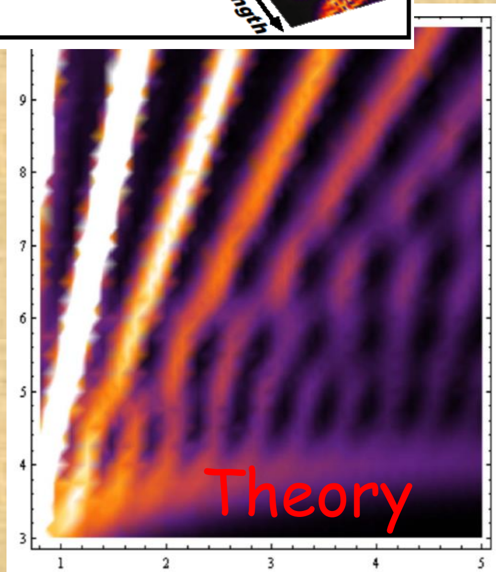

Neutrons tunneling through the mirror

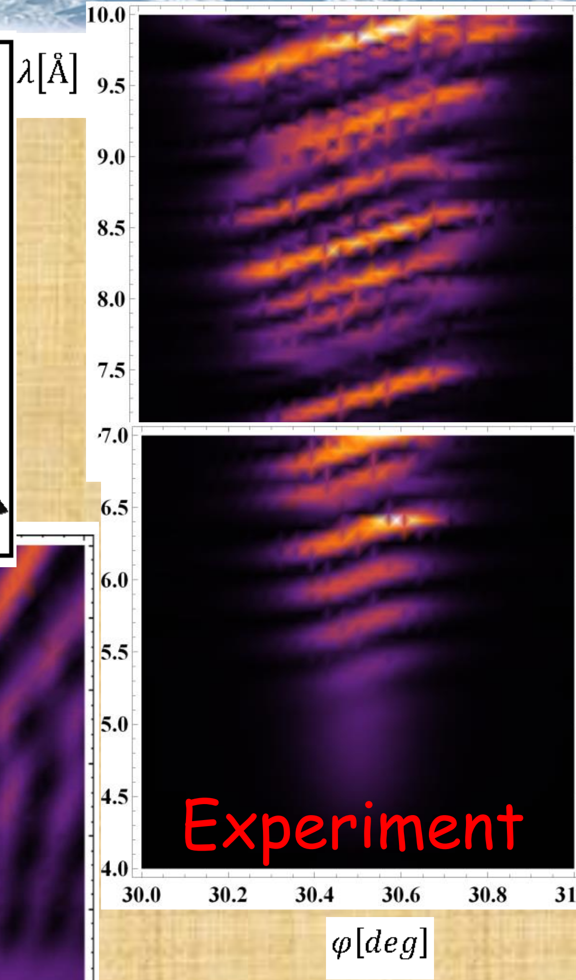

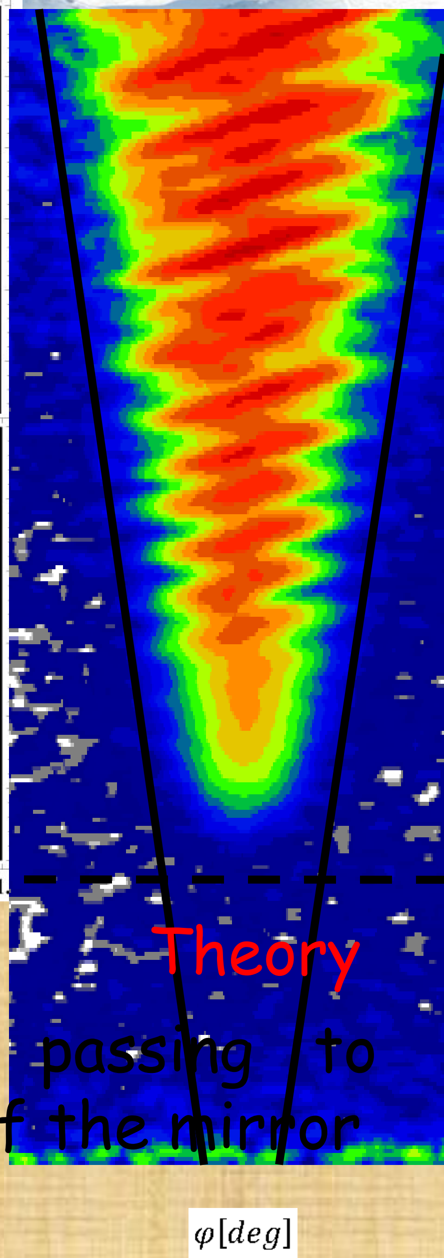

Neutrons passing to the exit of the mirror

Short-range forces. More recent improvements

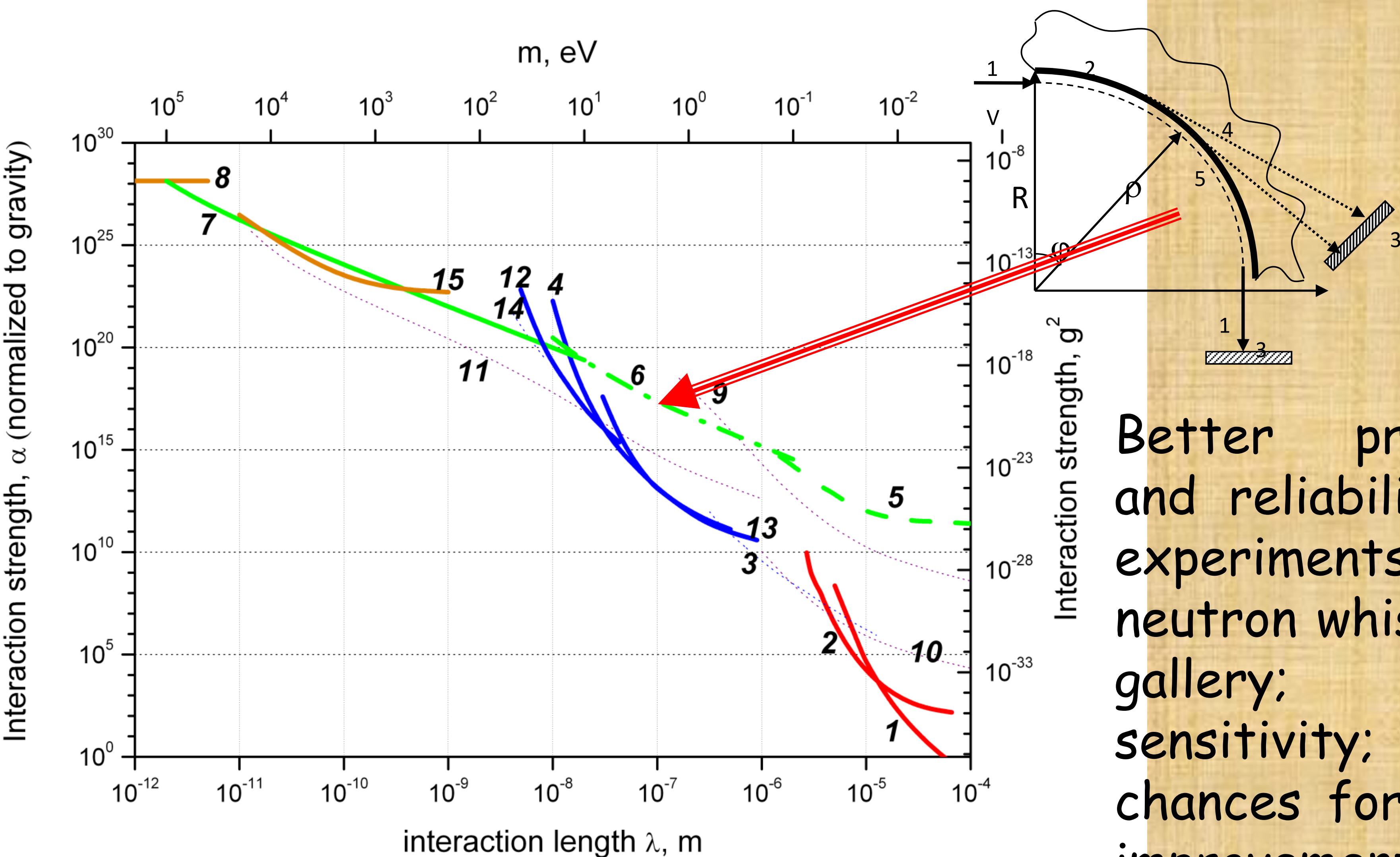

Better precision and reliability for experiments with neutron whispering gallery; record sensitivity; good chances for major improvements

New experiment with a MgF2 concave mirror

Improvements:

- No Si-oxide layer on the mirror surface (as in the preceding experiment), thus better defined surface potential and smaller systematics;
- Lower impurities on the surface, and thus smaller systematics;
- Suppression of parasitic transitions between whispering-gallery states due to the more uniform surface potential;
- Optimization of the neutron beam shaping and resolutions, thus higher statistics and lower systematic effects;
- Better control of the false effects due to the major experience gained with Si mirrors;
- Higher critical velocity of the mirror material, thus the access to shorter distances also higher statistics.

New experiment with a MgF2 concave mirror

NEUTRONS FOR SCIENCE

Raw data

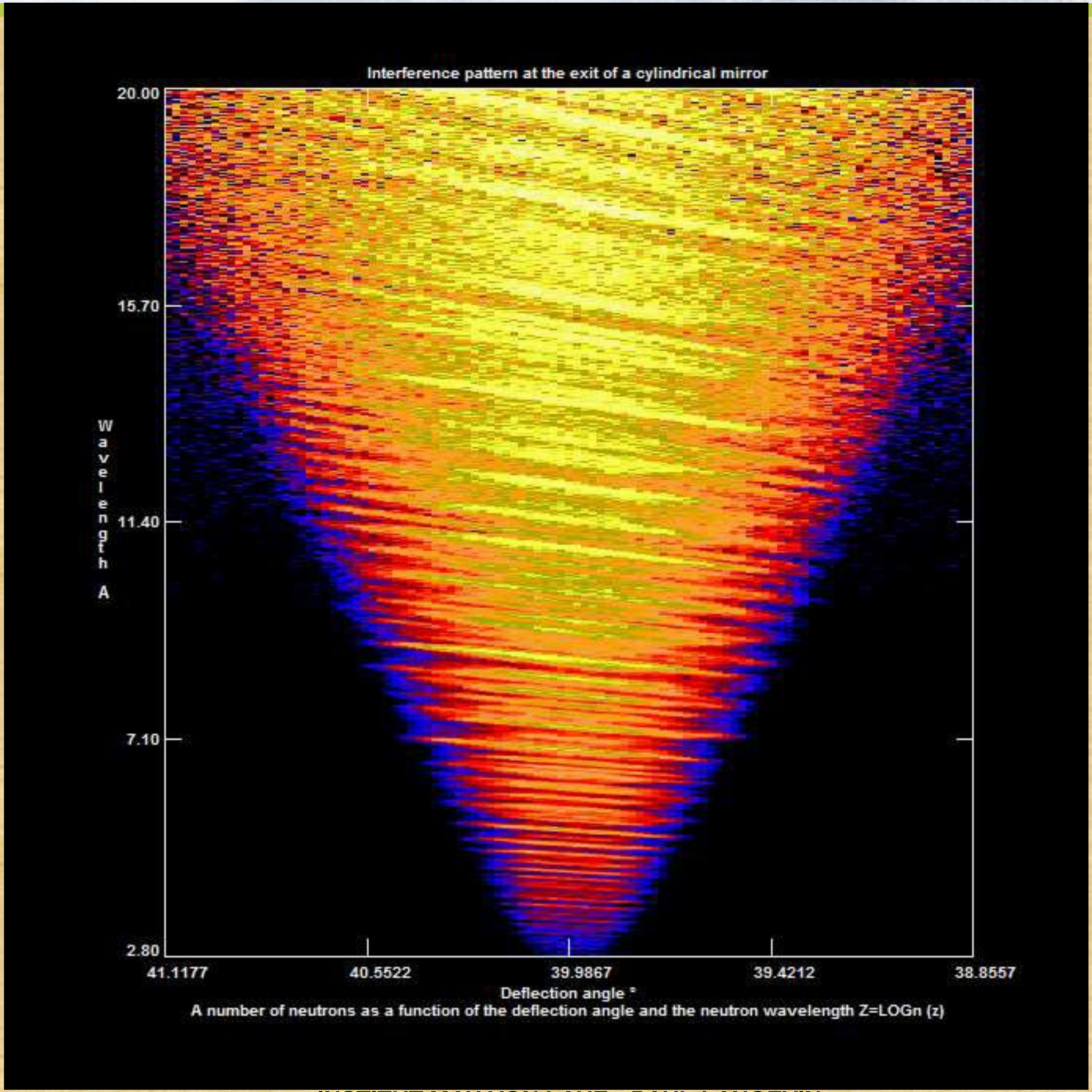

New experiment with a MgF2 concave mirror

Examples of the data/calculations

Analysis of the data is in progress

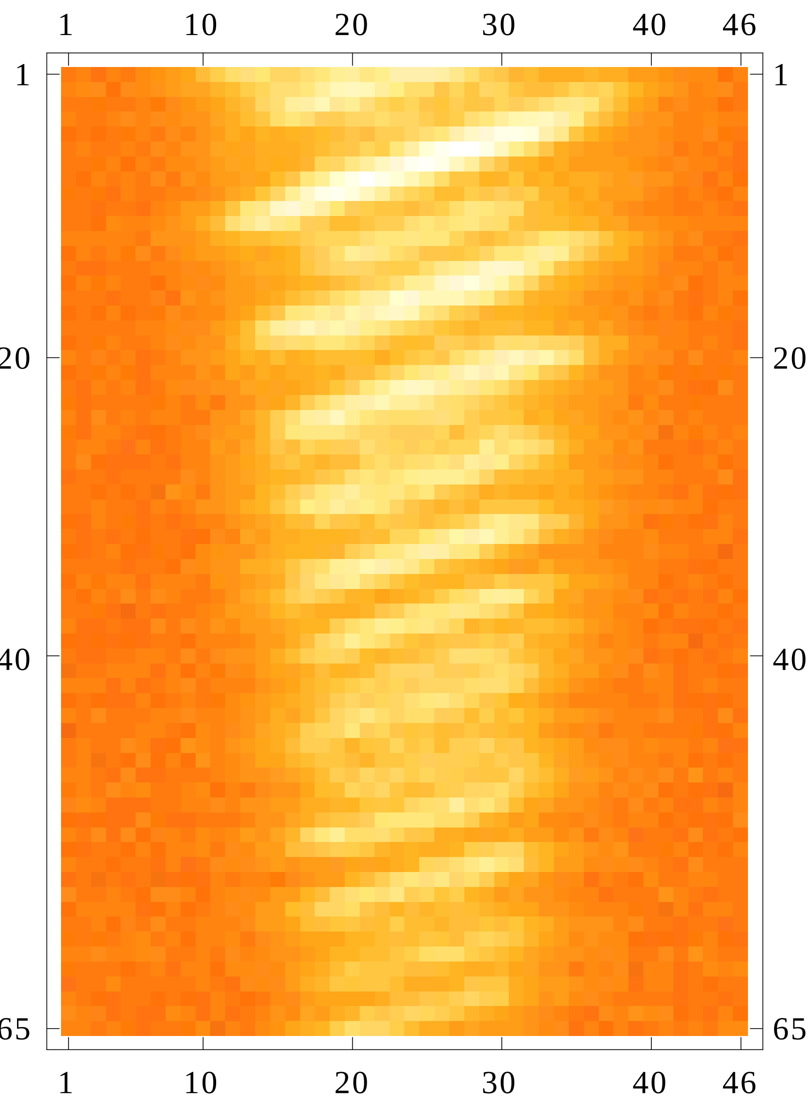

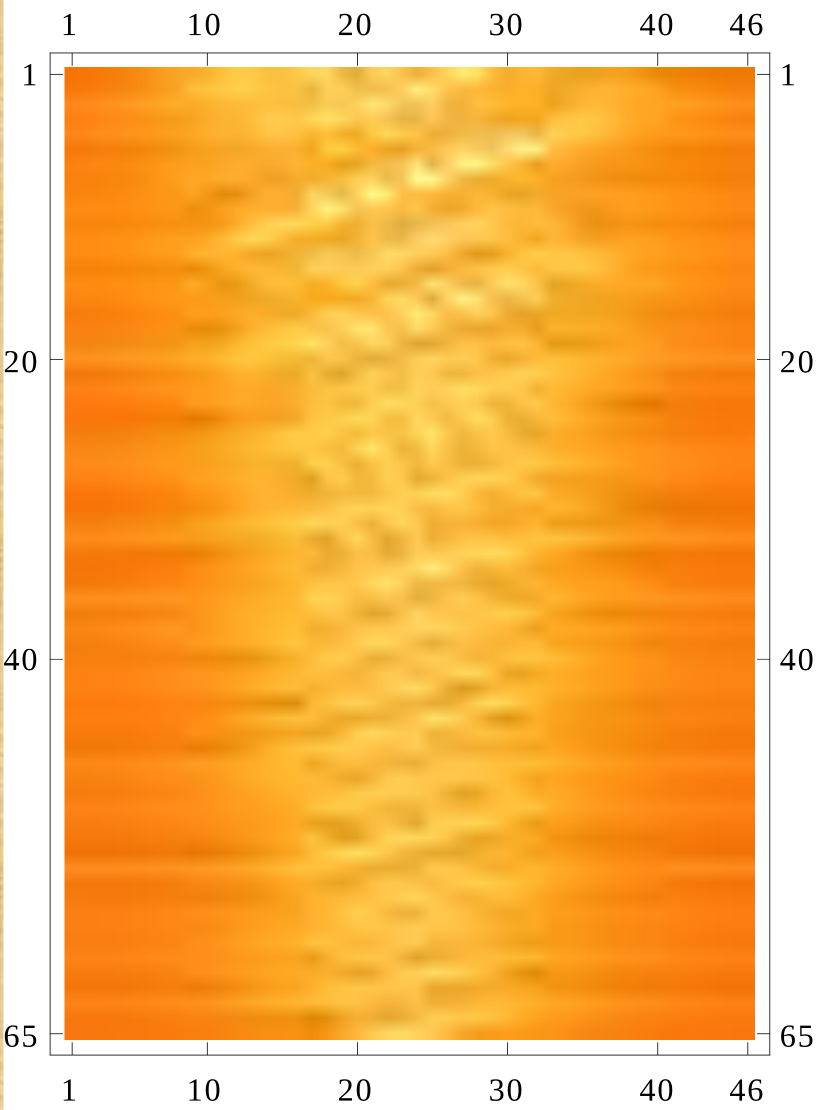

New experiment with a MgF2 concave mirror

Examples of the data/calculations

Analysis of the data is in progress

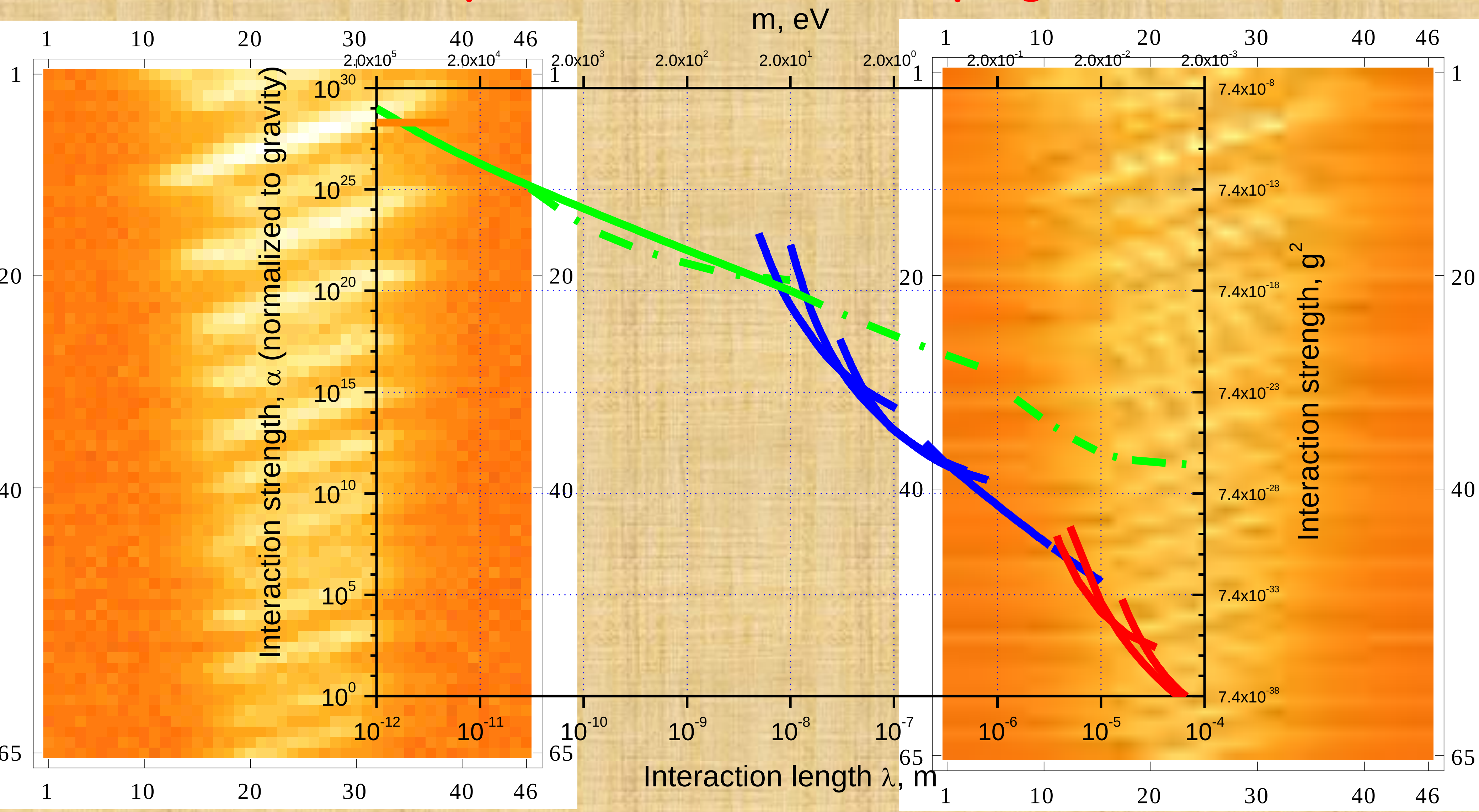

Conclusion

- The method of quantum bouncing is gaining ground, attention and support. It is powerful, can be "**easily**" implemented;

- Neutron (neutron-related) constraints for fundamental short-range interactions are **improving** in a broad distance range due to efforts of different groups using different methods;

- All these activities are **efficient** in terms of results/resources;

- These tendencies will stay for the observable **future**.

after Conclusion

Gravitational states of $\bar{H}(H)$ atoms on the He surface in at fall

$$\tau_{H,\bar{H}}^{gr.1} = \frac{\hbar}{2gbm_{n,H,\bar{H}}} = 1.35\ s \qquad t_0^{gr.} = \frac{\hbar}{\varepsilon_0^{gr.}} = \sqrt[3]{\frac{2\hbar}{g^2 m_{n,H,\bar{H}}}} = 0.46\ ms \qquad \frac{\Delta\varepsilon^{gr.}}{\varepsilon^{gr.}} \sim \frac{t_0^{gr.}}{\tau_{H,\bar{H}}^{gr.}} = 3.4 \cdot 10^{-4}$$

$$\frac{\Delta g}{g} \sim 10^{-6}$$

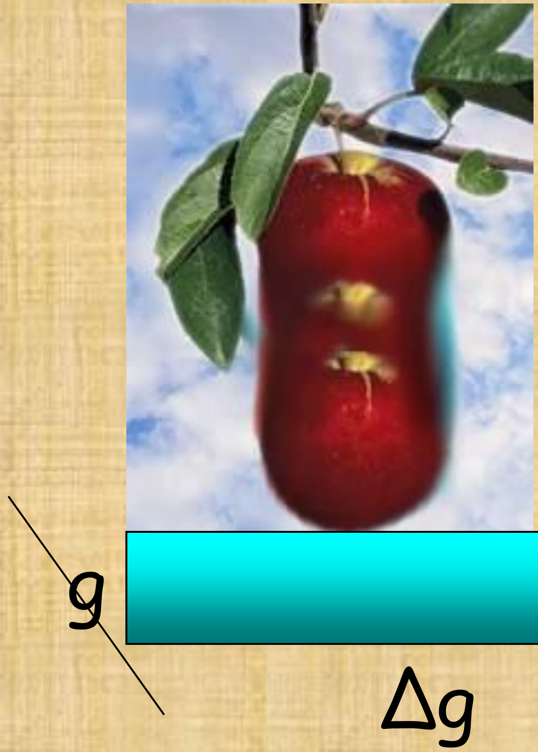

$$\tau_{H,\bar{H}}^{\Delta gr.} = \frac{\hbar}{2(\Delta g)bm_{n,H,\bar{H}}} = 1.35 \cdot 10^6\ s \qquad t_0^{\Delta gr.} = t_0^{gr.} \cdot \sqrt[-1,5]{\frac{\Delta g}{g}} = 4.6\ s$$

$$\delta_{st.}^{GBAR} \frac{t_0^{\Delta gr.}}{\tau_{H,\bar{H}}^{\Delta gr.}} \sim 0.03 \cdot \frac{4.6}{1.36 \cdot 10^6} \sim 10^{-7}$$

$$\sim 10^{-7} \cdot 10^{-6} \sim 10^{-13}$$